2024 HAMDA RAFIQUE MSCHW-F22-038 FOS

Synthesis Of Copper Selenide Aerogel For Photoreduction Of Carbon Dioxide

SUPERIOR UNIVERSITY

Thesis Submitted to

The Superior University Lahore

In Partial Fulfillment of the

Requirement for the Degree of

M.Phil Chemistry

By

HAMDA RAFIQUE

SU92-MSCHW-F22-038

Session: 2022-2024

Faculty of Sciences

Synthesis Of Copper Selenide Aerogel For Photoreduction Of Carbon Dioxide

SUPERIOR UNIVERSITY

Thesis Submitted to

The Superior University Lahore

In Partial Fulfillment of the

Requirement for the Degree of

M.Phil Chemistry

By

HAMDA RAFIQUE

SU92-MSCHW-F22-038

Session: 2022-2024

Faculty of Sciences

Author's Declaration

I hereby state that my MS/MPhil thesis titled **"Synthesis of copper selenide aerogel for photoreduction of carbon dioxide"** is my work and has not been submitted previously by me for taking any degree from this University,

The Superior University, Lahore

or anywhere else in the country/world.

At any time if my statement is found to be incorrect even after my graduation, the university has the right to withdraw my M.Phil. degree.

Name of Student: Hamda Rafique

Date: _____

Plagiarism Undertaking

I solemnly declare that research work presented in the thesis titled **"Synthesis of copper selenide aerogel for photoreduction of carbon dioxide"** is solely my research work with no significant contribution from any other person. Small contribution/help wherever taken has been duly acknowledged and that complete thesis has been written by me.

I understand the zero-tolerance policy of the HEC and University,

The Superior University, Lahore

towards plagiarism. Therefore, I as author of the above-titled thesis declare that no portion of my thesis has been plagiarized and any material used as a reference is properly referred/cited. I undertake that if I am found guilty of any formal plagiarism in the above-titled thesis, even after awarding of MS/M.Phil. degree, the University reserves the rights to withdraw/revoke my MS/M.Phil. degree and that HEC and the University have the right to publish my name on the HEC/University website on which names of students are placed who submitted a plagiarized thesis.

Student/Author Signature: _____

Name: Hamda Rafique

Research Completion Certificate

This is to certify that the thesis entitled **"Synthesis of copper selenide aerogel for photoreduction of carbon dioxide"** submitted by **"Hamda Rafique"** has been accepted towards the partial fulfillment of the requirement for M.Phil. **"Chemistry"**. The quality of the work contained in this thesis is adequate for the award of degree.

Supervisor Name: Dr. Fizza Naseem
Designation: Assistant Professor

Signature: _____

Certificate of Approval

This is to certify that the research work presented in this thesis, titled **"Synthesis of copper selenide aerogel for photoreduction of carbon dioxide"** was conducted by **"Hamda Rafique"** under the supervision of **"Dr. Fizza Naseem"**

No part of this thesis has been submitted anywhere else for any other degree. This thesis is submitted to the Faculty of Sciences, The Superior University, Lahore in partial fulfillment of the requirements for the degree of Master of Science/Master of Philosophy in the field of "**Chemistry"** in Faculty of Sciences at The Superior University, Lahore.

Student Name: Hamda Rafique Signature: _____

Examination Committee:

Session Chair: Dr. M. Mudassir Iqbal Signature: _____

a) External Examiner: Dr. Iqra Muneer Signature: _____
   Assistant Professor
   Department of Chemistry
   University of Engineering and Technology, Lahore

b) Internal Examiner: Dr. Shaukat Ali Signature: _____

c) Supervisor Name: Dr. Fizza Naseem Signature: _____

d) Name of HOD: Prof. Dr. Uqba Mehmood Signature:_____

e) Name of Dean: Prof. Dr. Mohammad Naveed Babur Signature:_____

f) Controller Examination: Dr. Muhammad Haris Signature:_____

Dedication

In the name of **Allah**, The Merciful, The Compassionate

First and foremost, I am deeply grateful to Almighty Allah for granting me the strength, patience, and wisdom to complete this thesis. His countless blessings have guided me throughout this journey.

I would like to express my heartfelt gratitude to my respected **supervisor** Dr. Fizza Naseem, who has supported me every day and guided me through this challenging task. Her unwavering encouragement, insightful feedback, and dedication have been invaluable in shaping this research. This project would not have been possible without her support and expert guidance.

Lastly, I extend my sincere appreciation to my family members for their unconditional love, patience, and support. Their constant prayers and encouragement have been my greatest source of strength throughout this academic endeavor. Without their encouragement, I would not have been able to complete this endeavor.

Acknowledgments

First and foremost, I bow my head in gratitude to **Allah Almighty**, the Most Gracious and the Most Merciful, whose countless blessings, guidance, and mercy enabled me to complete this M.Phil. journey. Without His divine will, strength, and wisdom, this accomplishment would not have been possible. In moments of difficulty, it was His light that guided me, His strength that uplifted me, and His mercy that comforted me. Every step of this academic pursuit has been a testament to His presence in my life, and I wholeheartedly dedicate this humble work to Him.

I extend my deepest and most sincere gratitude to my beloved **parents**, whose love, patience, and unwavering support carried me through this journey. Their sacrifices—both financial and emotional—have been the foundation of every success I have achieved. They stood beside me through every challenge, offering words of comfort and motivation when I was low, and sharing in my joy at every accomplishment. Their prayers were my shield, and their trust in my abilities gave me the courage to keep going. I dedicate this work to them with profound respect and love.

I am deeply thankful to my respected **supervisor Dr. Fizza Naseem**, who played a vital role in shaping this research with patience, wisdom, and immense dedication. Despite my shortcomings and moments of negligence, she continued to support, guide, and mentor me with remarkable tolerance and kindness. Each discussion and piece of feedback contributed significantly to my academic growth. The knowledge, discipline, and critical thinking that I developed under her supervision have been invaluable. I am sincerely grateful for her belief in me and consistent encouragement throughout this journey.

Last but not least, I dedicate this thesis to my **dear friends**, who continuously encouraged me and believed in my ability to complete this work, even when I doubted myself. Their constant moral support, kind words, and motivation helped me stay focused and optimistic. Whether it was through late-night conversations, shared laughter during stressful times, or quiet companionship, their presence made this journey less daunting. I am thankful for their encouragement, which served as a reminder that I was never alone in this endeavor.

Hamda Rafique

Table of Contents

Page

Author's Declaration……...II

Plagiarism Undertaking……..III

Research Completion Certificate……..…….IV

Certificate of Approval……V

DEDICATION…….....VI

ACKNOWLEDGEMENTS…….....VII

TABLE OF CONTENT…...…….....VIII

LIST OF TABLES…….....XI

LIST OF FIGURES…….....XII

LIST OF ABBREVATIONS…….....XIII

ABSTRACT…….....XIV

CHAPTER 1…….....01

INTRODUCTION …….....01

1.1 Background of Aerogel…….……01

1.2 Properties of Aerogel…….……02

1.3 Silica Aerogels…….……..04

1.4 Increasing emission of CO_2…….…….....05

1.5 Photoreduction of CO_2…….....06

1.6 Photoreduction of CO_2 through Aerogels……..…….……...07

1.7 Copper Selenide Aerogel…….....08

1.8 Properties of Copper Selenide Aerogel……...09

1.9 Photocatalytic Process…….……09

AIMS AND OBJECTIVES…….....11

CHAPTER 2 …….....12

LITERATURE REVIEW…….....12

CHAPTER 3 …….....23

METHODOLOGY……..... 23

3.1 Materials…….....23

3.2 Apparatus…….....23

3.3 Procedure…….....23

3.3.1 Synthesis of copper selenide aerogel…….……23

3.3.2 Synthesis of CuO/CuSe AG……..…….……...….....24

3.3.3 Photocatalysis for Carbon Dioxide Reduction…….……..24

CHAPTER 4…….....26

RESULTS …….....26

4.1 Optical Properties…….……26

4.1.1 Ultraviolet-Visible Spectroscopy……26

4.1.2 Photoluminescence…….…..……...27

4.1.3 Fourier Transform Infrared Spectroscopy……29

4.2 Morphological Properties……..……..…….…..30

4.2.1 Scanning Electron Microscope…….....30

4.3 Structural Properties……...…...….32

4.3.1 X-ray Photoelectron Spectroscopy……..…….…...32

4.3.2 X-ray Diffraction…….…….…...33

4.4 Photocatalytic carbon dioxide reduction into methanol……..…..35

4.5 Gas Chromatography……..….37

CHAPTER 5 …….....40

DISCUSSION…….....40

CHAPTER 6…….....42

CONCLUSION …….....42

REFERENCES…...…….....43

List of Tables

Description **Page**

Table 4.4 GCFID Signals data……38
Table 4.5 Comparison of yield of CuSe and CuO@CuSe AG……..……39

List of Figures

Description **Page**

Figure 1.1 Properties of Aerogels 2

Figure 1.2 Properties of copper selenide..... 9

Figure 3.1 Diagrams of Aerogel before and after calcination……25

Figure 3.2 Photocatalytic Chamber..... 25

Figure 4.1.1 (a) Comparison UV Graphs of CuSe AG and CuO@CuSe AG..... 26

Figure 4.1.1 (b) Comparison Band Gap of CuSe AG and CuO@CuSe AG..... 28

Figure 4.1.2 Comparison PL Graphs of CuSe AG and CuO@CuSe AG..... 30

Figure 4.1.3 Comparison IR Graphs of CuSe AG and CuO@CuSe AG 31

Figure 4.2.1 SEM images of (a) CuSe AG (b) CuO@CuSe AG 32

Figure 4.3.1 XPS Graphs of (a) Survey scan of CuO@CuSe AG (b) O1s, (c) Cu 2p3/2 and (d) Se 3d 32

Figure 4.3.2 XRD Graph of composite CuO@CuSe AG 35

Figure 4.4 Figure 4.4 Comparison of Methanol analysis chromatogram via Gas Chromatography (a) GC methanol Standard data chromatogram (b)) Methanol chromatogram CuSe AG (c) Methanol chromatogram of CuO@CuSe AG……..37

Figure 4.5 Comparison Yield Graphs of CuSe AG and CuO@CuSe AG..... 39

List of Abbreviations

AG	Aerogel
QDs	Quantum dots
IUPAC	International Union of Pure and Applied Chemistry
NASA	National Aeronautics and Space Administration
VOCs	Volatile Organic Compounds
CB	Conduction band
VB	Valence Band
NPs	Nano particles
FE	Faradaic Efficiency
USFT	Ultrasonication and reflux heating
CFs	Cellulose Fibers
NOx	Nitrogen oxides
PEC	Photoelectro-catalytic
SWE	Subcritical water extraction
GO	Graphene Oxide
UV	Ultra-Voilet
PL	Photoluminescence
FTIR	Fourier transform Infrared Spectroscopy
XPS	X-Ray Photoelectron Spectroscopy
SEM	Scanning Electron Spectroscopy
XRD	X-ray diffraction

ABSTRACT

Aerogels are recognized as remarkable materials because of their fine, inorganic superstructure with high porosity. Aerogels are generally characterized by high surface areas leading to increase the amount of available active sites for CO_2 adsorption. High porosity of aerogel makes reactant diffusion easier, which lead to higher catalytic efficiency. Optimized structures of copper selenide aerogel can promote fast dynamics of charge carriers, reducing losses through recombination and increasing overall performance. Through sol-gel method, copper selenide aerogel and through co-precipitation method copper oxide dopped copper selenide aerogel was prepared. Different characterization techniques such as SEM, XPS, FTIR, UV-visible spectroscopy and XRD was applied to analyze the morphology and structural features of the copper selenide aerogel. Synthesized aerogel was used as photocatalyst in CO_2 reduction, and its ability in reduction of CO_2 was tested under controlled conditions. Gas chromatography is utilized to analyze the resulting gas product such as methanol. The resulting CuSe AG and CuO@CuSe AG demonstrated a methanol yields of 81.057 μmol g^{-1} h^{-1} and 1046.63 μmol g^{-1} h^{-1} respectively, and an optical band gap of 1.53 eV was achieved from the doping of CuO into CuSe aerogel. These properties highlight the material's enhanced light harvesting and catalytic performance, making it highly suitable for applications in photoreduction of CO_2.

CHAPTER 1

INTRODUCTION

1.1 Background of Aerogel

The first aerogels were made in 1931, in order to drain a wet gel of its liquid. Historically, the process of gel drying involved the liquid evaporating in air. Interfaces between liquid and vapor forming the gel network produced a surface significant shrinkage due to tensions, because of a partial network collapse, after drying. When the gel structure became sufficiently strong to withstand the high tensile strength of the fluid [1]. Aerogels with a variety of remarkable properties which pique the interest of academics in diverse fields of technologies and science. Their applicability spectrum is nearly infinite, making their way through various branches like absorption of kinetic energy, insulation against heat and sound among other fields, biomedicine, chemistry, electronics, and optics etc. [2-6]. They're nanoscopic materials having characteristics smaller than ten nanometers, a monolith that is several centimeters in size overall. They might be insulating or conductive, clear or completely black, incredibly effective or chemically inert catalysts, vibrant and magnetic, luminous, and super absorbers [7]. It is important to define the term "aerogel" first because literature frequently takes a variety of approaches. Aerogel is regarded as "Affinity gel represents a microporous solid substance containing gas as the dispersed phase " by the IUPAC Gold Book, which uses zeolites, microporous glass, and microporous silica as examples. This definition proves restrictive because it addresses microporous materials with pores falling below 2 nm only. The definition excludes traditional silica aerogels together with other substances because their pores measure between several nanometers and many tens of nanometers. Accepted knowledge shows that aerogels exist as porous open frameworks which have nanoscale characteristics with both mesoporous structure and small macropores alongside high surface areas exceeding 100 m^2 g^{-1} and high porosity rates reaching at least 90% [8].

Aerogels with high thermal insulation have a wide range of industrial applications, including energy, buildings, civil engineering, subsea systems, cryogenics, space, and the environment. Aerogels have garnered significant attention in the academic and industrial communities worldwide over the last twenty years due to their excellent

physical properties, controllability, and broad range of applications. Furthermore, due to their geometrical morphology, aerogels' super-thermal-insulation properties lead to limited thermal conduction by the gas voids and a dissipative pathway for heat transport by the low solid content under phonon scattering. Due to their inherent brittleness and low mechanical strength, silica aerogels have been commercialized extensively for thermal insulation purposes; however, they fall short of the stringent requirements of extreme industrial fields. According to NASA, the 21st century will see just as much use of aerogels as plastic. Consequently, it is imperative to concentrate on optimizing various aspects associated with aerogel manufacturing, including production expenses, ecological safety, and, above all, the augmentation of mechanical strength as shown in fig 1.1. The main obstacle to aerogels' industrialization has long been acknowledged, despite the enormous efforts made to develop them. This obstacle is the extension of their excellent properties into the nanoscale [9].

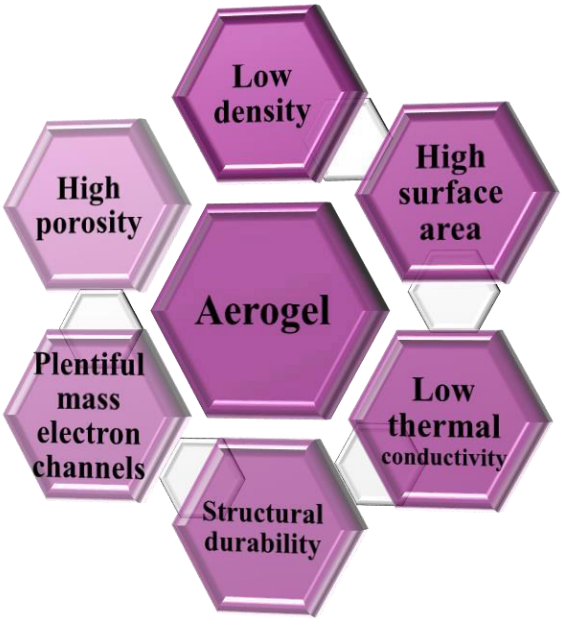

Figure 1.1 Properties of Aerogel

1.2 Properties of Aerogel

Aerogels are composed of bonded, flexibly packed fragments or fibrous material that are inflated throughout their magnitude by a gas, giving them an open, non-fluid viscous or polymeric matrix with a very low thickness and a high specified surface zone. Typically, an initial gel is formed by eliminating all swell agents without

significantly reducing its volume or compaction of the network [10]. The microstructure, which is made up of tiny pores, connected primary particles, and the fundamental solution chemistry can be used to modify composition through a procedure called the sol-gel method. Because of this distinctive microstructure, these thin materials show a variety of peculiar and intriguing qualities. Actually, aerogels possess the minimum thermal conductivity, refractive index, and sound velocity and the dielectric constant of every tested solid [2]. An aerogel is a material composed of organic, inorganic, or composite precursors that is produced by replacing the liquid in an alcogel with a different liquid using the sol-gel process and fast dehydrating technology, resulting in the formation of a three-dimensional, incredibly spongy network. Customizing aerogel's composition and network structure is made feasible by the sol and gel process. By preparing aerogels, drying step is the most crucial because it determines the final structure's morphology, porosity, and structural integrity [11]. In addition to being lightweight and having customized mechanical properties, aerogel/epoxy composites can offer controlled thermal, electrical, and dielectric properties. The final density and porosity of the aerogel are determined by ligament thickness. Aerogels made of silica, alumina, and carbon are currently accessible. The potential to create aerogel/epoxy composites for insulation, create aerogel-based active biosensors, and create lightweight, low-dielectric materials [12].

Aerogels provide a wide range of potential uses in high-tech, textile, environmental, and energy conversion and storage fields. The intriguing characteristics of aerogel fibers, such as their fire-retardant, mechanical, thermal and optical qualities. Furthermore, covered are new developments in the fields of artificial muscles, information storage, water harvesting, shielding, smart wearable fabrics, thermal management, and shielding [13].

One of the current directions in the development of green and low-carbon building materials is the use of the carbonization curing process to prepare building materials. It is theoretically possible to enhance the amount of CO_2 adsorption during the carbonization curing process by using aerogel in the production of carbonized curing building materials. This would enhance the effect of carbonization curing and eventually improve the performance of carbonized curing building materials. Building materials will have both good thermal insulation and carbon capture

capabilities if the aerogel mixture can achieve large-scale CO_2 capture. This will give the materials their functionalized and environmentally friendly qualities [14].

1.3 Silica Aerogels

The production process of silica aerogels involves extracting the liquid from silica gels through supercritical methods in order to create their three-dimensional silica particle networks. Space missions need thermal insulation materials that use silica aerogels because these materials exhibit fundamental characteristics such as low density and minimum thermal conductivity. Silica aerogels become brittle when exposed to low compressive forces. The right choice of silane precursors and polymer reinforcement result in more robust aerogels with increased strength and stiffness [15]. The silica precursor system forms a silica network containing reaction condensation water combined with alcohol-filled pores as the main liquid component. The possible monolith structures developed after drying and liquid phase removal of gels include aerogel, xerogel and nonporous monolith. The silica aerogel shows distinctive physicochemical properties through its undamaged 3D silica network after the drying process [16].

Silica aerogel exists as a nanostructured material which possesses an extensive specific surface area. reduced dielectric constant, high porosity, low density, and superior heat insulation qualities. Silica aerogels display distinctive properties which include 500–1200 m^2/g specific surface area and 80–99.8% porosity together with a density of 0.003 g/cm^3 and thermal insulation value of 0.005 W/m K and ultra-low dielectric constant (k= 1.0 – 2.0) and low index refraction (1.05) [17].

The production of silica aerogels follows these three fundamental procedural steps: (1) sol-gel gel preparation that requires aging the gel solution in its original solvent to avoid later drying-induced contraction and (2) gel processing under precise conditions to maintain structure integrity and (3) nanoscale sol particles are formed spontaneously in the precursor solution or are catalyzed by catalysts through hydrolysis and condensation reactions [18].

1.4 Increasing Emission of CO_2

The greenhouse effect triggered heightened interest about accelerating CO_2 emissions within atmospheric levels. Laboratory testing indicates aerogels would be suitable for CO_2 capture because they possess very high surface area (>800 $m^2.g^{-1}$) coupled with proven primary mesoporosity (20–50 nm) and their high permeability (~95%) makes them attractive for this application [8,9]. The increase of atmospheric CO_2 functions as the primary driver of global warming creating possible risks for human existence. The global shortage of energy resources limits progress on CO_2 emission reduction through environmental talks that are currently taking place between international parties. The solution requires innovative technologies because these issues compete against each other [19].

Conversion of CO_2 into methanol through photocatalysis efficiency benefits from multiple advantages. Fossil fuel control and global warming concern are both important yet the present production levels of methanol remain low. The catalyst material trial preparation procedure needs further improvement. Research shows various catalysts can be used for photocatalytic processes yet aerogels remain one of the most recognized nanostructured materials because they possess elevated porosity and low density and significant specific surface. Particle size serves as another helpful instrument for lowering internal diffusion resistance of reaction molecules because of aerogel [20,21].

Water and air pollution difficulties have become severe in modern societies because heavy industries continue to grow rapidly while climate patterns decline. Multiple pollutants including heavy metals and organic dyes and NOx and VOCs have received extensive environmental research during the recent years. The recently identified pollutants tend to be toxic and cancer-causing substances that produce harmful effects on both ecosystems and public health. People believe it is essential to create both cost effective and effective approaches to eliminate environmental pollutants [22]. The release of (CO_2) serves as a leading greenhouse gas that triggers climate change alongside global warming effects. A cost-efficient environmentally friendly procedure for both converting and utilizing CO_2 requires immediate development. CO_2 stands as the most stable thermodynamic carbon compound because its C double bond O Bond energy E = 803 kJ/mol (298.15 K) and its standard enthalpy of formation equals

– 393.5 kJ/mol. Energy consumption needs to reach significant levels to activate CO_2 due to its high thermodynamic stability. Thermal catalysis along with traditional methods demonstrates poor effectiveness for the task. The reductions of CO_2 become feasible through artificial photosynthesis when implemented under mild operational conditions. The development of CO_2 photoreduction processes needs stable photocatalysts capable of turning CO_2 into useful fuels among ethanol methanol formaldehyde methane and formic acid. Among the main barriers preventing selective CO_2 photoreduction toward CH_4 lies in the complex nature of protonation step [23]. CO_2 gas stands as the main source responsible for greenhouse gas emissions. Different countries propose cutting down the share and complete quantity of coal alongside other primary fuels and reducing energy usage and maintaining enhanced energy efficiency while generating clean power systems and actively working on emission reduction. Petrochemical energy powered by coal is expected to continue holding a substantial portion of the energy market during the next foreseeable period. Figure demonstrates CO_2 emissions from worldwide energy production between 1990 and 2020. Natural energy utilization since the past 30 years has produced expanding carbon emission levels [14].

The global CO_2 emissions in 2021 from fossil fuel usage in buildings amounted to 8% of total releases while electricity and heat energy usage and building construction materials production responsible for 19% and another 6% respectively [24].

1.5 Photoreduction of CO_2

Aerogels possess extremely large surface areas ranging from 500 to 1200 m^2/g that provide numerous active sites which boost the effectiveness of CO_2 photoreduction. The porous nature of aerogels (more than a 90% porosity) allows efficient gas diffusion and permits CO_2 molecules to easily bind with the active sites of the material [25].

The excellent thermal insulation capabilities of aerogels enable them to protect reaction temperatures from loss thus helping to preserve optimal photoreduction conditions. Such optical materials can be engineered to achieve specific properties consisting of minimal refractive index together with remarkable transparency. Light absorption occurs when combined with improved photoreduction performance [26].

Since the 18th century, environmental contamination has gotten worse, having a major negative impact on the environment, society, and economy. This is mostly because of the rapid population growth and widespread use of coal and petroleum. Greenhouse gas emissions, which include CO_2, are steadily increasing. The use of fossil fuels, especially coal, oil, and natural gas, as well as soil erosion and deforestation are human-caused sources of greenhouse gas emissions. These gases are principally to blame for global warming due to their capacity to create a greenhouse effect. The average temperature has risen by about one degree Celsius since the preindustrial era, and this trend is anticipated to continue. Because of its steady annual increase in the atmosphere, one of the main chemicals released has contributed to climate change: CO_2. A few of the climate issues it has raised are rising sea levels, shifting tides, and extreme weather, all of which put the long-term survival of human civilization at jeopardy. A fast expansion of sustainable power solutions offers a solution to solve current worldwide issues between limited resources and environmental destruction. Utilizing boundless solar energy allows CO_2 to function as a valuable material for producing formic acid and other compounds. This chemical compound maintains high stability because its carbon-oxygen double bonds have a dissociation energy value of $\sim$750 kJ mol^{-1} that exceeds the bond strengths of carbon hydrogen ($\sim$430 kJ mol^{-1}) and carbon-carbon ($\sim$336 kJ mol^{-1}) single bonds. A substantial quantity of energy is essential to unravel CO_2 before transmuting it into other chemical substances. A variety of chemical and biological and electrochemical and thermochemical and photochemical pathways exists which converts carbon dioxide (CO_2) into alcohols and light hydrocarbon products. The reduction of carbon dioxide by photocatalysis stands out as a strong alternative approach to multiple other technologies when achieving clean fuel and industrial gas production. When semiconductor materials receive sunlight activation this leads to pollution reduction in the atmosphere. Energy-intensive molecules such as CO, methanol, formaldehyde, methane and many more chemical compounds can be produced through carbon dioxide utilization as the most viable method [27].

1.6 Photoreduction of CO_2 through Aerogels

The chemical stability of aerogels allows researchers to customize them for CO_2 photoreduction through different materials including metal oxides, carbon, and silica. The integration of composites with fragile aerogels produces materials that become

mechanically sound for photoreduction system applications [28]. The semiconductor photocatalyst activates photochemical reactions after receiving artificial or natural light belonging to ultraviolet or visible wavelengths. Science refers to this reaction method as photocatalysis. The technology operates while saving money while producing zero environmental impact. The use of photocatalysts occurs when semiconductors function as the key element exposed to light waves exceeding or matching their bandgap energy values. The discovery of various solar-active catalysts for CO_2 photoreduction exists although they show instability and high selection rates alongside low conversion rates and deficient water suppression during hydrogen evolution [27].

1.7 Copper Selenide Aerogel

Various geometrical configurations of CuSe exist as rare metal chalcogenides alongside CuSe, Cu_2Se, Cu_2Sex, $CuSe_2$, and Cu_2Se etc. Metal chalcogenides demonstrate special characteristics which make them suitable for photocatalytic applications and thermoelectric conversion as well as gas sensors and solar cell performance. Semiconductors composed of CuSe exhibit their principal application in destroying organic chemicals through photochemical reactions. The P-type semiconductor material Cu_2Se exists in orthorhombic and monoclinic and cubic crystal forms. Cu_2Se stands out as an appealing active photovoltaic material because it accommodates wide ranges of crystal structures and particle sizes and band gap matches [29].

Photocatalytic technology has gained increased attention recently because it shows great promise as an environmental cleanup solution and hydrogen development system and carbon dioxide reduction method. The main atmospheric cause of greenhouse effects arises from CO_2 emissions that keep increasing at a speed which presents multiple severe risks like global warming [30-32]. CO_2 functions as the primary greenhouse agent leading to global warming that may trigger 2.4°C-4.5°C global temperature increases. Gas properties of CO_2 stability together with inertness lead to a Gibbs free energy formation value of ΔG_f 298° = -394.36 kJ/mol. Additionally the substance requires extensive energy through high pressure or temperature conditions to convert it into other products. Scientists and technologists

consider the conversion of CO_2 under benign conditions as one of the most crucial and difficult subjects of modern science [33].

1.8 Properties of Copper Selenide Aerogel

Photocatalysis demands a semiconductor material that exhibits the right bandgap which is copper selenide. The material exhibits light-absorption properties that generate electron-hole pairs for starting redox reactions. The photo-created electrons from the semiconductor reduce CO_2 into various hydrocarbon products or alternative useful chemicals. The properties of copper selenide aerogels become modifiable through adjustments made to synthesis parameters including precursor concentration together with solvent selection and drying process. The adjustable properties of this material make possible the optimization for maximum photo reactivity performance. Maximum catalytic efficiency of the aerogel occurs through combined selenium with copper because of their synergistic properties as shown in fig 1.2. Selenium molecules have two positive effects on aerogel electrical behavior and light reaction properties [34].

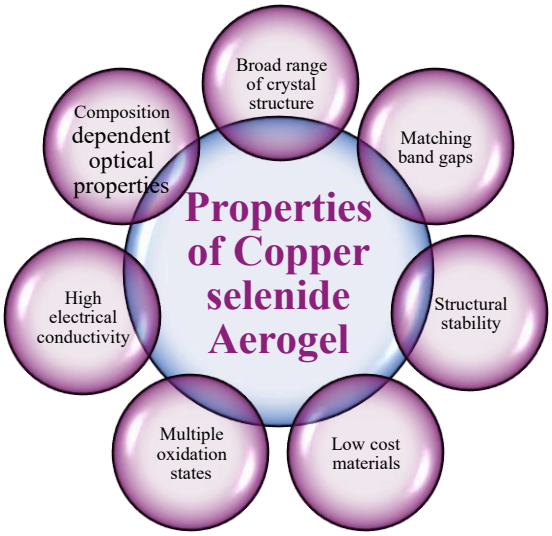

Figure 1.2 Properties of copper selenide aerogel

1.9 Photocatalysis Process

The CO_2 reduction takes place through electrocatalysis together with photocatalysis as the two primary approaches. Through absorbing light energy, the catalyst drives valence band electrons to separate as holes and electrons. The catalyst surface accepts reduction and oxidation triggers which remain from valence band holes while

electrons move to the conduction band. Since the previous twenty years research has identified TiO_2 and CuO as metal oxide photocatalysts and also metal sulfide photocatalysts alongside additional material types [35].

Light photons use their band gap (E_g) equal to or exceeding the semiconductor catalyst (SC) to separate electrons (e^-) from holes (h^+) so both move into the empty valence and conduction bands (CB and VB). Different redox cycles initiated by these powerful electric charge carriers consecutively generate the final products [36].

AIMS AND OBJECTIVES

- To synthesize copper selenide aerogel
- To characterize copper selenide aerogel
- To investigate the structural and optical properties of the synthesized product
- To access the photocatalytic efficiency of copper selenide aerogel to reduce CO_2

CHAPTER 2

LITERATURE REVIEW

Guocan Jiang et.al prepared the quantum dots (QDs) aerogel. During aerogel manufacture some organic ligands including mercaptoacids remain bonded to the gel surface while blocking the photocatalyst functions. A new method was developed to address this limitation by using the inorganic ligand $(NH_4)_2S$ without sacrificial agents which delivered CdSe QD aerogel with a very high carbon monoxide production rate at 15μmol $g^{-1}h^{-1}$ [37].

Aerogel material made of Bi-Sn served as the catalyst for electrochemical CO_2 reduction to methanol. The maximum faradaic efficiency (FE) amounting to 93.9% of Bi-Sn aerogel results from its advantageous transport capabilities and enhanced accessibility of active sites [38].

Xinxin Xiao et.al developed carbon-based aerogels containing copper nanoparticles through electrolytic reduction of carbon dioxide into carbon-based fuels. The carbon dioxide reduction process faces inefficiency issues because of the strong carbon dioxide bond (C=O, 806 KJ mol^{-1}) and the competing evolution reaction contributes to hydrogen gas formation in moist environments. Electrochemical reactions utilize copper (Cu^0) as an efficient electrochemical catalyst for this application yet its stability problems together with low selectivity rates remain its main issues. The CO_2 conversion generates better outcomes when utilizing metal-based catalysts comprising copper components. Carbon aerogels have become a central focus in electrocatalysis research because they offer strong advantages related to high specific surface area alongside many active sites. The stability of Cu NPs for effective CO_2RR improves when the metal forms alloys with AuCu and CuPt because this combination enables less than 45% FE for CO and CH_4 production [39]. The electrocatalytic behavior of the Mo-Bi bimetallic chalcogen system (MoS_2/Bi_2S_3) has been evaluated by Xiaufo Sun et.al who showed that 71.2% Faradaic efficiency for methanol production could be obtained at a current density of 12.1 mA/cm^{-2}. However, low current density and FE value remained a main limitation [40].

The research team of Dexin Yang studied copper selenide nanocatalysts for their use in electrochemical CO_2 reduction into methanol. The electrocatalytic reduction of CO_2 to methanol demanded both slow kinetic and complex six-electron/proton coupling procedures [40]. Three main issues in such reactions include low current density combined with poor selectivity along with high overpotential. Extremely robust electrocatalysts require rational design for large-scale implementation because they should produce high current density and high selectivity. Under electrochemical conditions Copper selenide nanocatalysts efficiently reduce carbon dioxide to methanol while reaching an exceptional 285 mV down overpotential alongside a 41.5 mA cm^{-2} high current density and a 77.6% FE. The catalyst operates with a selectivity of 77.6%. The catalyst performs methanol production through the balanced interaction between copper and selenium elements. The electrochemical properties excel because copper selenide shows high electrical conductivity and multiple oxidation states. The open Se atoms surrounding the structure enhance both activity site exposure and electrical conductivity and reduction ability of CO_2 because of their unsaturated nature [41]. Research by M. Le et.al shows that electroreduction of CO_2 into methanol achieves highest promise with catalysts based on copper and precious metals. Reports indicate that among reactant materials Cu demonstrates superior efficiency as a selective electrocatalyst for CO_2 reduction into alcohols and hydrocarbons even though bulk Cu exhibits subpar activity and selectivity when producing methanol [42]. The existing reported catalysts show moderate current density and selectivity rates but current density and FE performance remain challenging to achieve together throughout the CO_2 to methanol conversion process. The scientific community and practical world share great curiosity about designing effective catalyst for improving performance and reducing overpotential while enhancing FE.

The electroreduction of carbon dioxide to methanol could be performed using Pd-Cu bimetallic aerogels. Pd-Cu aerogel served as an effective electrocatalyst because its $Pd_{83}Cu_{17}$ aerogel structure features a three-dimensional network of wire-like components which enabled 80.0% Faradaic efficiency and 31.8 mA cm^{-2} current density at an overpotential of 0.24 V [43]. I will manufacture an aerogel composed of copper and selenium to perform efficient photoreduction operations

on CO_2. As copper selenide contains inexpensive accessible elements it serves as an environmentally friendly sustainable choice for carrying out CO_2 photoreduction. Copper selenide aerogels require stability and extended service life for their application as long-term photoreduction materials.

The synthesis of PbSe nanostructured gels occurs through a sol-gel method where nanoscale particles assemble until CO_2 supercritical drying produces aerogels. The elimination process of the PbSe thiolate-capped nanoparticles produced a gel structure instead of forming a colloidal precipitate through careful management of thiolate removal. Nanoparticles of sphere-shaped PbSe formed when precapping methods were used yet the postcapping approach generated cube-shaped nanoparticles through the synthesis process. Two distinct morphologies linked to the nature of nanoparticles emerged as a colloidal gel network (pearl-necklace) through sphere particles while cube-shaped nanoparticles enabled a hierarchical gel network to occur. The measurements revealed a blue-shifted band-gap in PbSe gels both when they had a spherical shape as well as when they had a cubic shape. The nano-particles adhere to quantum confinement principles of bulk PbSe particles. Xerogels show a lower surface area compared to aerogels which indicates their reduced density and higher porosity and this property fully contributes to aerogels' quantum confinement when compared to xerogels [44].

Zhian Zhang et.al developed 3D interconnected mesoporous carbon aerogels (MCA) encapsulated selenium sulfide (SeS_2) to build composite materials for lithium batteries through carbon and selenium sulfide combination. The lithium-sulfur battery's low performance output arises from its insulating nature along with electrolytic and electronic properties as well as dissolved organic electrons and the soluble reductive polysulfides. The technique requires highly efficient conducting porous carbon as a host to both minimize intermediate polysulfide formation and enhance sulfur cathode conductivity. Selenium stands as a sulfur congener because scientists have evaluated it for lithium battery applications that require high energy density due to better electrical conductivity than sulfur alongside comparable volumetric possibilities. Different applications besides lithium-ion batteries have required the production of Aerogels [45].

Alexander et.al conducted research on metal and transition oxide-based aerogel production. Alexander et.al thoroughly examined epoxides as a gelation agent which enabled the synthesis of chromia aerogels and xerogels from chromium inorganic salts. The researchers combine various solvent proportions with salt concentrations when making these aerogels. The method proved successful but the chosen gelating agent lacks affordability as well as accessibility. Manufacturing these special epoxidebased aerogels needs extensive time and expenditure because epoxides possess both rare application and high-cost properties [46].

Scientists extensively study and implement silica aerogels because they have exceptional properties that include high surface area along with low density and excellent thermal insulation abilities. The thermal insulation and high degree of porosity representing 99.8% are the defining features of silica aerogels. Their framework provides low refractive indices since they are also lightweight materials. Aerogels find use in catalyst applications as well as thermal insulation and acoustic insulation roles and additional uses needing materials with high surface area properties [47]. Building thermal insulation materials of high efficiency become increasingly popular among the construction industry. Research has introduced nanomaterials as silica aerogels to create renders with thermal conductivity measurements under 0.030 $W\ m^{-1}\ K^{-1}$. Efforts to use aerogel suffer from two major limitations due to their highwater absorption rate through capillaries and low mechanical strength properties.

The combination of aerogel with fibers produced improved mechanical strength together with reduced water uptake throughout capillary action but maintained low thermal conductivity when compared to the render without fibers. The characteristics displayed wide variations between organic fibers and synthetic fibers. The research stands out because it determines aerogel-based fiber-enhanced thermal renders can improve energy efficiency both for new buildings and retrofit projects. The implemented resources provide direct solutions to the climate emergency [48].

The research by Pedro A.V. Freitas examined cellulose aerogel production from purified rice straw cellulose fibers (CF) through extraction methods which combined subcritical water extraction (SWE) at 160 and 180°C and conventional alkaline treatment (ALK). The investigators developed a new water-based extraction technology which incorporated ultrasonication and reflux heating (USHT) in the process. The characteristics together with the chemical composition of rice straw cellulose fibers were significantly altered during the purification procedure. The USHT treatment proved equally proficient in removing silica from the fibers as ALK treatment while the CFs retained approximately 16% hemicellulose content. Selective hemicellulose removal during SWE extractions improved notably when using temperatures of 180°C along with 3% of SWE but the elimination of silica at 15% was less efficient. Changes in CF composition produced different properties during hydrogel formation as well as affected the aerogel characteristics. The aerogels showed more cohesive structure with thicker walls and higher porosity rate and water vapor absorption ability but presented a reduced ability to hold liquid water (0.2 g/g). Better hydrogel structures formed from CF materials due to its elevated hemicellulose fraction that improved its water retention properties. Aerogels and hydrogels developed into less structured structures because of silica content leftovers which produced fibrous materials with lower porosity (97–98%) and also affected their formation process [50].

Spinning processes at various speeds emerged according to the rate at which building blocks need to organize themselves in a sol–gel state. Engineers can direct the mechanical properties of aerogel fibers during manufacturing for bending purposes and additional applications that include knotting and twisting abilities along with weaving capability and even artificial muscle resemblance. Wearable clothing uses properly collected or woven aerogel fibers to act as effective materials against heat loss [51].

Recent studies about graphene-based aerogels focus on their interesting properties which include suitable anchoring positions and flexible shape-transforming capabilities and adjustable functional groups and pore sizes while also showing great potential for toxic pollutant removal. The possible water and air pollution management solutions using graphene-based aerogels have been thoroughly

studied and reported. At the beginning of the presentation the Scientist demonstrated contemporary research demonstrating aerogels made from graphene operate as sustainable materials which decompose both heavy metal ions and organic dyes while purifying water and atmospheric air from volatile organic compounds (VOCs) and nitrogen oxides (NOx). The article details multiple structural modifications of graphene aerogels which play a vital role in improving adsorption and catalysis properties. The potential of graphene-based aerogels as environmentally functional materials attracted Bin Gao to present the current challenges and available prospects for their industrial development [52].

Ceramic aerogels demonstrate excellent potential to serve as protective materials alongside thermal insulators in extreme conditions. Current synthesis methods do not provide economic conditions that permit high-throughput non-oxide ceramic aerogels production at an affordable price using minimal time and energy consumption for future large-scale manufacturing. Lujia Han demonstrated a method to produce SiC aerogels at a volume ranging from 1000% to a liter capacity during standard laboratory experiments at a manufacturing rate of 16 L/min. To achieve effective large-scale applications and high-throughput production it is vital to optimize both combustion synthesis along with the conversion process from powder to aerogel products with large volume increases above 1000%. The synthesis procedure needs minimal energy and operates independently. This product has an exceptionally cheap price tag that amounts to \$0.7 L^{-1} (\$7 kg^{-1}). The synthesized SiC aerogels showcase important thermal and mechanical properties that include extreme flexibility and reduced heat flow and the ability to resist damage. The proposed innovation requires examining combustion synthesis as a method for converting raw materials directly into bulk functional products while establishing viable techniques to industrialize ceramic aerogels production [53].

Photoreduction of CO_2 into valuable fuels proves to be an effective method for balancing global carbon reserves using solar power from renewable sources. Scientists face substantial obstacles while devising affordable and active yet highly selective and stable photocatalysts to reduce CO_2 into useful products. Xiaodong Wu synthesized the novel SiOC aerogel photocatalyst using heat

treatment and supercritical drying on the one-step sol-gel method. The photocatalytic performance enhancement stems from the SiOC aerogel formation whose BET specific surface area is large accompanied by typical hierarchical structures. Experimental findings showcase the formation procedure leading to SiOC whisker aerogel development. Under simulated sunlight conditions the optimized SiOC aerogel generates 5.8 and 20.5 μmol/g of CH_4 and CO through photochemical reactions without requiring additional co-catalysts or sacrificial agents. The activity levels of the pristine SiC aerogel fall short of those obtained from the aerogel by factors of 3.9 and 6.4. Analyzing the density functional theory (DFT) results shows that the produced SiOC aerogel effectively binds and activates CO_2 and H_2O molecules when they interact with the catalyst surface. The SiOC aerogels demonstrate superior catalytic behavior than pure SiC and SiO_2 clusters according to the rate-determining step calculations and Gibbs free energy diagram analysis. The efficient CO_2 reduction depends on both the excellent structural properties and electronic structure modification which accelerates the separation and transfer of charge carriers. The research demonstrates a new approach to design photocatalysts through its simultaneous power to activate CO_2 from aerogel-based porous materials together with carrier separation capability [54].

According to Prabhu Saravanan et.al Titanium dioxide (TiO_2) remains a leading research subject for CO_2 photoconversion because it offers lower costs and superior stability together with non-toxic properties among other photocatalysts. The only condition that activates pure TiO_2 exists through exposure to ultraviolet (UV) light. The reduction of CO_2 with PEC (Photoelectrocatalytic) process utilizes various metal oxide photocatalysts. As a whole the current photocatalysts show inadequate quantum efficiency levels. Scientists have attempted different approaches to enhance photocatalysts by adding metal elements as well as nonmetallic components and linking them with secondary semiconductors. Purposes of photocatalysts become better with carbon materials participation because carbon provides superior electrical properties coupled with increased surface area. Scientific research demonstrates that the superior properties of carbon-based together with aerogel (AG) catalysts elevates PEC CO_2 reduction efficiency levels [55].

Hsiang Tseng generated methanol in photochemical carbon dioxide reduction of aqueous solutions under 254 nm irradiation. Homogeneous hydrolysis served as part of an improved sol-gel process for developing titania and Cu-loaded titania materials. The prepared TiO_2 and Cu/TiO_2 nanoparticles displayed an average size of approximately 20 nm with a uniform distribution of the grains. UV lamp fitted in the middle of a quartz reactor served as the platform for photocatalytic reduction activities. A catalyst dispersion maximum was achieved through the use of 2.0 weight percent copper loading. The production of methanol from 2.0 weight percent Cu/TiO_2 materials under six hours of UV light reached 118 μmol/g. The yield of 250 μmol/g from the former exceeded the 4.7 and 38.2 μmol/g yields recorded by sol–gel TiO_2 and Degussa P_{25}. Solar irradiation exposure lasting 20 hours brought the methanol production to stabilize at 250 μmol/g. The experimental results showed that NaOH addition resulted in a substantial increase of methanol yield. The caustic solution dissolved a greater amount of CO_2 than plain water did. The aqueous solution contained OH^- which provided strong scavenging of holes as an additional function. The distribution of electric charge together with the $Cu\text{-}TiO_2$ Schottky barrier helps promote electron trapping through supported Cu. Photocatalytic efficiency of Cu/TiO_2 increased substantially because of diminished hole-electron pair recombination probabilities. The maximum energy and quantum efficiencies reached 10% and 2.5% respectively [56].

The reduced graphene oxide/cellulose-derived carbon composite aerogels were developed by Ruiwen Shu through a method which required high-temperature carbonization and chemical crosslinking. The original binary aerogels displayed two essential characteristics including a lightweight composition and a three-dimensional porous architecture that formed from chemical epichlorohydrin crosslinking. The electromagnetic parameters together with microwave absorption characteristics of composite aerogels changed dramatically because of varying weight ratios of graphene oxide (GO). The combination of GO at 1.5 mg/mL produced the most effective microwave dissipative binary composite aerogel. When using a 2.47 mm thick aerogel filled to 17.5 weight percent minimum reflection loss reached an exceptional -51.42 dB. The composite aerogel sample with 2.73 mm thickness extended microwave absorption across both X-band and

Ku-band frequencies with an effective absorption bandwidth reaching 7.28 GHz. A computer simulation method allowed researchers to analyze far-field contributions of binary composite aerogels toward radar cross section evaluations. The study presented a probable way that microwave signals get damped. The researchers expected their discoveries to function as a reference for developing effective and broad-spectrum microwave absorber carbon-derived composite aerogels [57].

Research into graphene derivatives for solar photocatalytic carbon dioxide (CO_2) reduction continues to grow because this approach offers suitable financial cost effectiveness together with dedicated resolution to resource management issues. Most investigations within this area overlooked the photocatalytic properties of graphene derivatives although they commonly functioned as co-catalysts. The study implemented heteroatom doping together with morphology modulation to synergistically improve the structure along with properties of graphene oxide (GO). A photocatalytic reduction of CO_2 occurred using an N,S-GOA three-dimensional graphene oxide aerogel that incorporated N and S dopants. The photocatalytic mechanism of N,S-GOA exposed CO_2 molecules under visible light to obtain carbon monoxide (CO) by functioning independently of co-catalysts or sacrificial agents. N and S co-doping enabled the formation of porous material with elevated specific surface area benefits because it promoted CO_2 adsorption alongside diffusion of products through the structure. This work presents both CO_2 adsorption applications and photocatalytic reduction functions alongside establishing a method for producing high-surface-area multi-active-site GO-based three-dimensional aerogels as photocatalysts [58].

The team of Hao Tang et.al focused their efforts on Au-CeO_2 composite aerogels by refining Au nanoparticle sizes because it involved crucial steps to develop heterojunctions between Au and semiconductors through surface plasmon resonance for photocatalysis enhancement. The new "plasmonic aerogel" photocatalyst implements Au nanoparticles of dimensions that approach those of the semiconductor phase. The research presents a novel approach toward controlling Au nanoparticles sizes in Au-CeO_2 composite aerogels that operates through the established epoxide addition sol-gel method framework. The mixed

organic acid additive containing a thiol group serves during gelation to perform size tuning by utilizing its multiple functionalities. The aerogel photocatalysts contain interconnected CeO_2 nanocrystals that join with Au nanoparticles having sizes spanning from ~30 nm to sub-10 nm and ~15-10 nm CeO_2 nanocrystals. The surface plasmon resonance peak position together with the peak intensity modification results from adjustments in the Au nanoparticle characteristics. The photocatalytic reduction of CO_2 from air to the solid surface serves as the evaluation reaction to assess the effects of Au nanoparticle dimensions on aerogel composite photocatalysts. Au nanoparticles result in a clear rise of overall activity for the CeO_2 aerogel photocatalyst. The extent of increase depends on the Au nanoparticle dimensions along with the products produced (CO or CH_4). A composite with smallest possible Au nanoscale dimensions provides the best performance results [59].

The research combined modified cellulose aerogels with steel slag freeze-dried material into a synergetic platform which supports water purification. Cellulose aerogels acquire better Cr (VI) removal properties thanks to their unique composition with steel slag active sites. Our experimental results demonstrate that composite aerogels treat Cr (VI) with outstanding performance since their visible light-mediated removal reaches 96.6% in 1 hour. Amino group protonation on the material surface attracts Cr (VI) anions through electrostatic interactions and photoproduced electrons from silicate compounds facilitate Cr (VI) reduction. This research advances environmental remediation composite material development through identification of valuable principles for designing advanced multiconcept water treatment systems. The research results demonstrate both innovative Cr (VI) contamination response techniques and environmentally-friendly practices.

Semiconductor (or co-catalyst) heterojunction interface engineering faces challenges due to their weak interactions in the structure. The protonation process strengthened the interface force between Bi_2MoO_6 with oxygen vacancy (OBMO) and graphene aerogel which in turn yielded a substantial enhancement of the Schottky heterojunction effect. The three-function applications of protonated OBMO graphene aerogel (p-OBMO/GA) include photodegradation of tetracycline along with H_2O_2 production and supercapacitor functionality. When

applied for H_2O_2 photocatalytic synthesis protonation has two benefits. It enhances the Schottky heterojunction interface performance and supplies protons which are directly involved in H_2O_2 creation. Computational methods verify that addition of protons benefits H_2O_2 synthesis since protons exist readily at the reaction site to erase the energy threshold needed for *OOH intermediate formation and reduce the barriers to H_2O_2 synthesis. The combined action of O vacancies and graphene co-catalysis creates numerous charge carriers and enhances the energy storage capacity through Schottky heterostructure junctions because protonation treatment optimizes the interface effect. The use of protonation treatment allows researchers to improve heterojunction effects through a newly discovered interface engineering methodology [60].

Research focusing on sustainable hydrogen supply methods concentrates on developing safe liquid hydrogen carriers with high hydrogen content because they require controlled storage mechanisms. Liquid hydrogen carrier dehydrogenation leads to extreme slow rates of hydrogen evolution which creates a substantial difficulty. The use of traditional accelerant additives in dehydrogenation reactions leads to a reduction in the maximum hydrogen storage capacity that can be achieved. Expert opinion identifies the task of attaining high efficiency hydrogen storage and release density as a complex problem. We have developed a photothermal activated suspended biphasic reaction process which absorbs sunlight then emits infrared radiation to cause photothermal evaporation and dehydrogenation of liquid hydrogen carriers without depending on additives. The phase transition-induced biphasic reaction design enables the strategy to raise reaction temperature needs but also reduces hydrogen transport resistance. When used as a pure chemistry formic acid drives hydrogen evolution by 386 mmol g^{-1} h^{-1} which reaches a storage density exceeding 53 g L^{-1} while surpassing modern practices by three times. Our method develops an innovative mechanism to dehydrogenate formic acid and hydrazine hydrate liquid hydrogen storage carriers and delivers superior hydrogen release performance and storage capability.

CHAPTER 3

METHODOLOGY

3.1 Materials

Copper sulphate dihydrate, Sodium selenide, distilled water, ethanol, Polyvinyl alcohol, TEOS, NaOH, HCl, copper nitrate trihydrate

3.2 Apparatus

Magnetic stirrers, beakers, volumetric flask, spatula, centrifuge machine for separating particles, autoclave or high-pressure reactor, supercritical drying apparatus, CO_2 cylinder, UV lamps or other light sources, gas chromatograph (GC) for gas analysis, characterization tools (SEM, UV-visible spectroscopy, FTIR)

3.3 Procedure

3.3.1 Synthesis of Copper Selenide Aerogel

Copper selenide aerogel was synthesized via the sol-gel method based on the reported procedure in literature with some modifications [61]. Total volume was 40 ml and reactant concentration were 2.5 mmol each. 0.05g of copper sulphate dihydrate was taken in 12ml of distilled water with continuous stirring for 2 minutes. Then, 0.05g of sodium selenide was added in 12ml of ethanol in another beaker. After that sodium selenide solution was added into the copper sulphate solution. Stir the above solution for about 10-15 minutes. 0.05g of PVA was added into 12ml of distilled water in another beaker with stirring. PVA solution was added dropwise into the above copper selenide solution. Color changed from sky blue to dark blue. Then, 4 ml TEOS was added into the above solution for formation of gel, and stirred the above solution for 15 minutes. After that, in order to maintain the PH to 7, NaOH solution was added dropwise. Then the sol was transformed into the molds and placed the beaker into water bath to maintain 0°C temperature. It left into the water bath for 3 hours. For gelation, the sol was then left for a week to convert into a gel. After a week, gel was formed. After formation of gel, the next step is to convert gel into aerogel. For this, the gel was soaked into ethanol several times to preserve its structure, and the gel was passed through freeze drying to remove all the solvent from the gel and made it an aerogel, the lightest of all gels. Then calcination took place at 750°C temperature for

3 hours. After calcination, crystalline phase of aerogel was obtained as shown in fig 3.1. Sample was then subjected to photocatalytic reduction.

Before Calcination **After Calcination**

Figure 3.1 Diagrams of Aerogel before and After calcination

3.3.2. Synthesis of CuO@CuSe AG Composite

Co-Precipitation method was applied for the synthesis of composite. 5g of copper selenide aerogel was added into 50 ml of distilled water with continuous stirring for 5 minutes. Then, took 5g of copper nitrate trihydrate in 50 ml of distilled water in another beaker. After that, CuSe Ag solution was added dropwise into the copper nitrate solution. Stirred the above solution for about 10-15 minutes. In order to maintain the PH to 14, NaOH solution was added dropwise. NaOH solution was prepared by adding 4g NaOH into 50 ml distilled water. After maintain pH, retain the solution at magnetic stirrer for 2 hours at 80°C temperature. Then, washed the above solution with distilled water and ethanol several times and dried it in a drying oven for 24 hours at 80°C. After drying sample was calcined at 500°C temperature for 3 hours. After calcination, nanoparticles of composite made, and used it for photocatalysis.

3.3.3 Photocatalysis for Carbon Dioxide Reduction

Photocatalysis of carbon dioxide (CO_2) is the process of using UV light to stimulate a chemical reaction that photo-catalytically transforms CO_2 into a useful product like methanol. Because the prepared aerogel absorbs photons from the light source and produces excited electrons and holes, it was used as a photocatalyst in this process. These excited electrons participate in the reduction of CO_2, whereas holes propel the oxidation of water to produce protons and oxygen. Fuels are created when CO combines with protons and excited electrons on the catalyst surfaces.

The figure 3.2 shows that 0.5g photocatalyst has been added in to 100 ml deionize water after all the setup completed, and put in to the flask. To do this, only the carbon dioxide was then passed and the solution was then magnetically stirred for 30 minutes. The zero sample was then collected by using a syringe transferred into the sample voil and then the UV lamp was opened after an hour 1st sample was collected temperature was 60°C the reaction continued for 2nd hour and then again 2nd sample was collected the reaction was continued for straight 6 hours and the sample was collected after every passing hour. After 6 hours, the reaction was then stopped, and the samples collected were then subjected to Gas Chromatography to measure the conversion of carbon dioxide into a useful product i.e. methanol.

Figure 3.2 Lab Build Photocatalytic Reaction Chamber

CHAPTER 4

RESULTS

4.1 Optical Properties

Optical properties were analyzed by using UV-visible spectroscopy (Agilent Technologies Cary 60), Photoluminescence spectroscopy (Florescence spectroscopy Agilent Cary Eclipse), and Fourier transform Infrared Spectroscopy.

4.1.1 Ultraviolet-Visible Spectroscopy

The composite exhibits at 564 nm, which is a notable shift from the absorption peak of 428 nm observed for pure copper selenide aerogel [62]. This redshift in the absorption peak suggests enhanced light harvesting capabilities, which is critical for applications in photocatalysis and solar energy conversion. The increase in absorption wavelength indicates that the composite may be more effective in utilizing visible light, thus improving its potential for photocatalytic CO_2 reduction as shown in fig 4.1.1 (a).

(a)

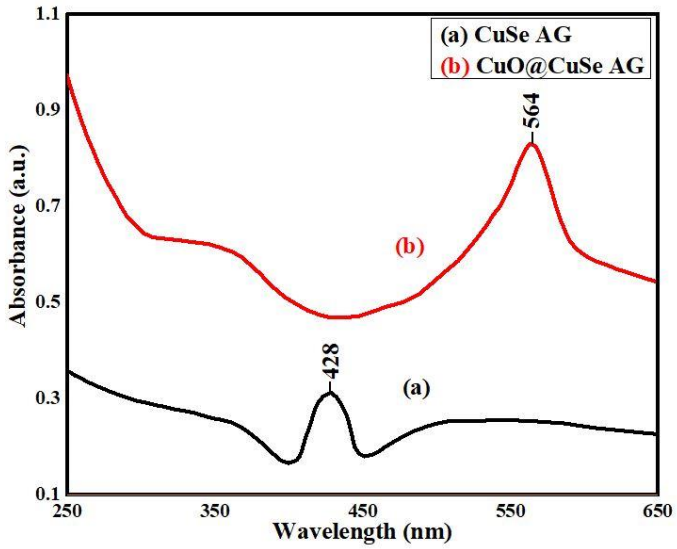

Figure 4.1.1 (a) Comparison UV graphs of CuSe AG and CuO@CuSe AG

The band gap of copper selenide aerogel was initially calculated to be 2.63 eV using the Tauc's equation, which is consistent with its known properties as a semiconductor.

However, after incorporating copper oxide into the composite, the band gap was reduced to 1.53 eV. This decrease in band gap is significant as it implies that the composite can facilitate electron transitions more readily, thereby enhancing its photocatalytic activity [63].

Moreover, the presence of copper oxide improves charge separation within the composite. Due to its high electrical conductivity facilitates electron transfer, reducing the recombination rates of electron-hole pairs generated during photocatalytic reactions. This synergistic effect between CuSe AG and CuO enhances the overall photocatalytic performance of the material as shown in fig 4.1.1 (b).

(b)

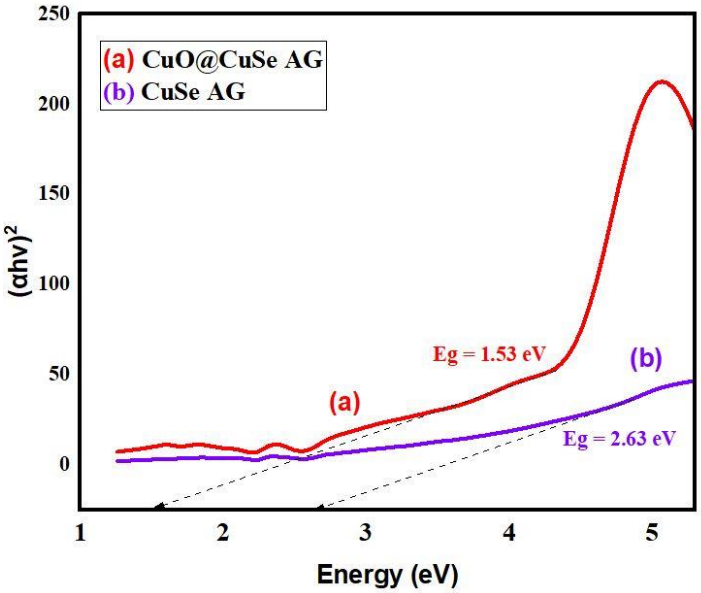

Figure 4.1.1 (b) Comparison Band gap graphs of CuSe AG and CuO@CuSe AG

4.1.2 Photoluminescence

Analysis of optical data the effectiveness of the transfer and separation of photogenerated charge carriers in the samples was examined using photoluminescence (PL) analysis. While a lower PL intensity peak indicates reduced recombination, larger PL emissions indicate a higher rate of electron-hole pair recombination. From the PL result of CuSe aerogel, there is absorption peak at about 533.5 nm and the optical emission band at 2.63 eV can be ascribed to the band-to-band recombination of CuSe. The optical emission band at 1.53 eV is due to the defect related recombination in CuO. Most importantly, the PL intensity of the CuO/CuSe

AG is higher than those of the pure CuSe AG, which can be ascribed to the efficient charge transfer and the carrier dynamics originating from the direct contact between CuSe AG and CuO in the composite as shown in fig 4.1.2.

CuO doping of PL Emission leads to newly created defect states which modify band alignment to decrease recombination energy. Improved electron trapping and delayed recombination creates conditions that enhance electron transfer because of the lowerenergy emission at 636.6 nm. The fast recombination of electron-holes in pure CuSe aerogel (533.5 nm) causes reduced efficiency during CO_2 reduction. The electron storage capability of CuO within CuSe AG at 636.6 nm wavelength decelerates recombination events and strengthens charge carrier splitting. The lower photon energy (636.6 nm) allows CuO-doped CuSe AG to absorb a larger range of visible spectrum. The number of photons leads to the production of additional charge carriers which facilitates CO_2 conversion. The heterostructure junction between CuO and CuSe AG enables efficient electron transport between the materials. CuSe AG electrons transfer to CuO crystals in order to reduce CO_2 while simultaneously reducing recombination losses. The vacancies serve as active centers which accelerate the electron transfer process of CO_2. When CuO doping happens in CuSe aerogel the photoluminescence wavelength shifts from 533.5 nm to 636.6 nm which demonstrates both improved charge separation capability and minimized recombination events and amplified visible light absorption. The improved electron transfer is enabled by this modification which prolongs carrier lifetime while also enhancing defect-generated active sites for effectively activating CO_2. The simple CuSe aerogel emits light at 533.5 nm while its restricted efficiency arises from fast recombination. The addition of CuO to CuSe AG resulted in wavelength-shift from 533.5 nm to 636.6 nm which led to reduced recombination reactions and better CO_2 reduction and charge transfer efficiency [64].

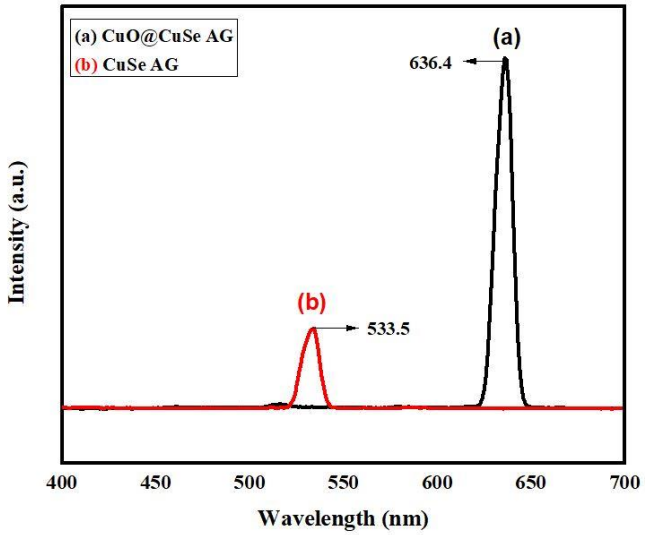

Figure 4.1.2 Comparison PL Graphs of CuSe AG and CuO@CuSe AG

4.1.3 Fourier Transform Infrared Spectroscopy

It is commonly recognized that every molecule or chemical structure exhibits a unique spectral fingerprint when exposed to infrared radiation. Thus, the functional groups of the produced samples were identified using FTIR spectroscopy. The synthesized CuO@CuSe AG composite's molecular structure and chemical composition were investigated using FTIR spectroscopy. From the FTIR spectrum obtained for the composite, several peaks that correspond to functional groups present in the composite were observed. The bands at ~544 cm^{-1} and ~836 cm^{-1} were assigned to Se-O and Cu-O stretching vibrations, respectively eligible for CuSe AG and CuO in the composite. Further, the FTIR data indicated some small peaks at around ~2838 cm^{-1}, which relate to O-H stretching vibrations that can be due to the adsorbed water or hydroxyl groups onto the surface of the composite [66, 67].

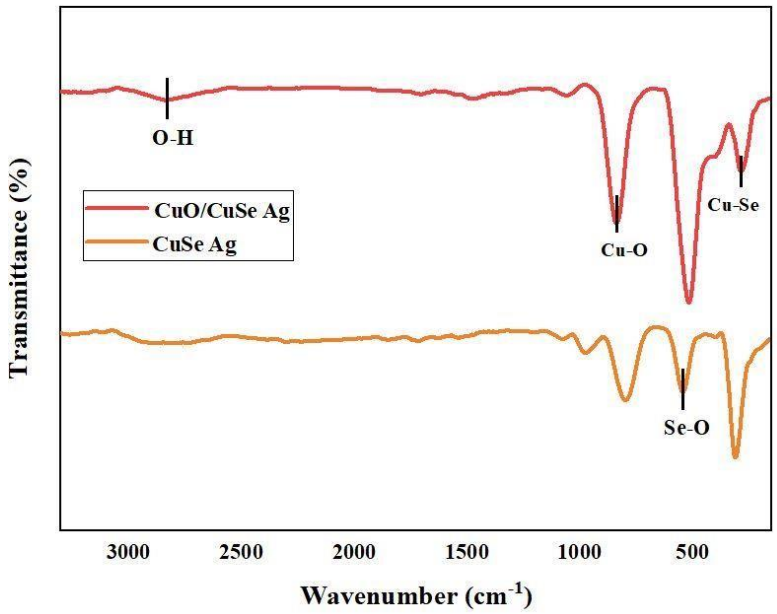

Figure 4.1.3 Comparison IR Graphs of CuSe AG and CuO@CuSe AG

4.2 Morphological Properties

4.2.1 Scanning Electron Microscopy

Morphological properties were analyzed by using Scanning electron microscopy (SEM). The morphology observed in SEM images are likely show a uniformly distributed copper-based nanoparticles. The size measurement of 180.60 nm suggests that composite has a significant degree of nanoscale features, which can enhance its reactivity and effectiveness in applications like photocatalysis. The interaction between CuO and CuSe is vital; it promotes charge transfer, which is essential for improving photocatalytic activity. The presence of CuSe aerogel may also contribute to this interaction by providing additional active sites for reactions due to its semiconductor properties [65]. Photo-catalytic effectiveness depends heavily on the porous aerogel structure because it generates an optimal surface area even when the dimensions measure 180.60 nanometers. Through its porous configuration this material obtains substantial catalytic active sites for effectively reducing CO_2 during photocatalytic reactions. Active dopants of copper oxide (CuO) enable the occurrence of two phases together in copper selenide (CuSe) frameworks. The SEM images show separate areas with distinct textures or contrast patterns which result from the phase

separation between copper oxide and copper selenide or heterojunction formation. A combination of heterojunctions within the material's structure allows better carrier charge separation and reduced recombination events to optimize photocatalytic reactions. The SEM analysis of copper oxide-doped copper selenide aerogel with 180 nm diameter should show a porous interconnected framework that ensures high surface area suitable for both CO_2 adsorption and photocatalytic reduction. The integration of copper oxide doping into copper selenide generates heterojunctions which helps split charge carriers to boost photocatalytic performance. Observations of the SEM data regarding particle distribution combined with morphology and copper oxide and copper selenide phase interaction patterns helps enhance material performance as shown in fig 4.2.1.

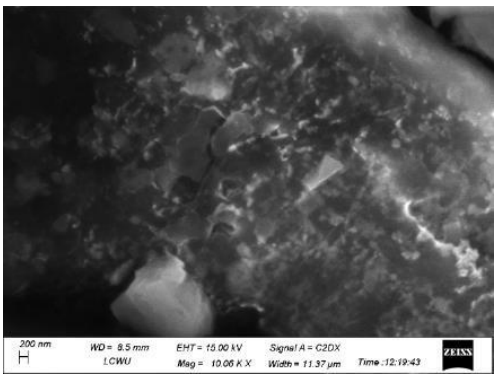

(a)

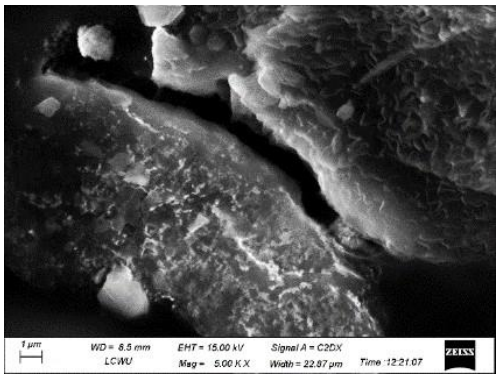

(b)

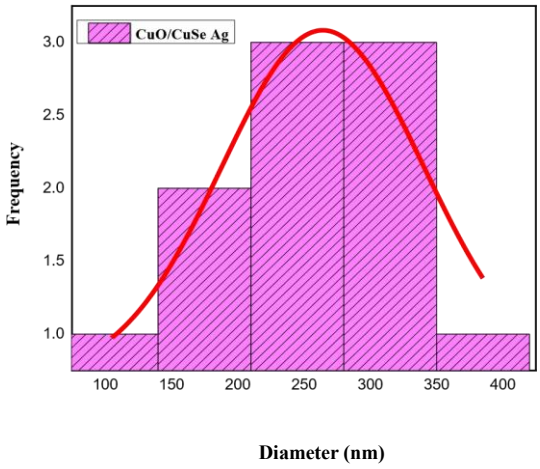

(c)

Figure 4.2.1 SEM images of (a) CuSe AG and (b) CuO@CuSe AG (c) Composite diameter

4.3 Structural Properties

4.3.1 X-ray Photoelectron Spectroscopy (XPS)

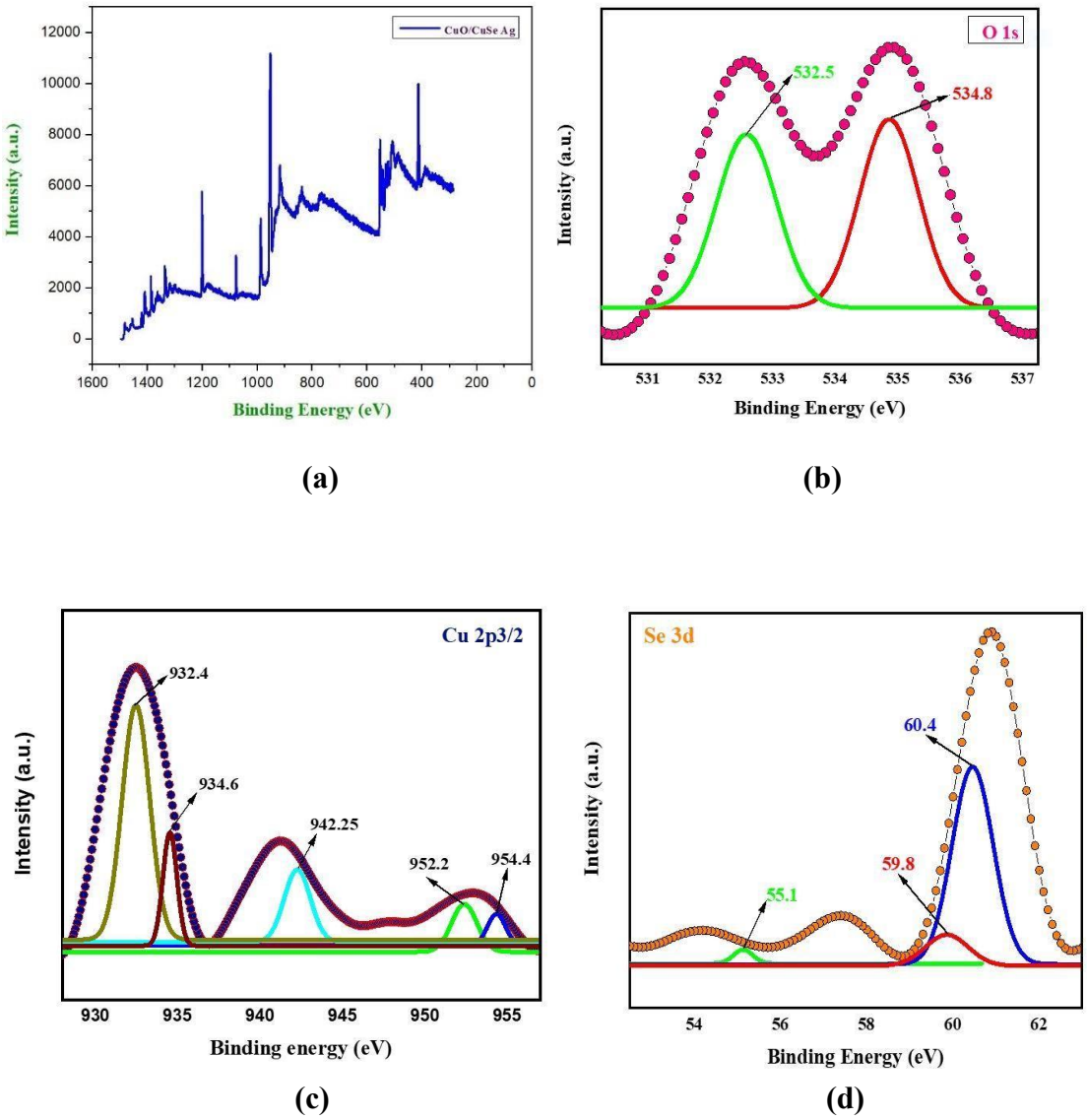

Figure 4.3.1 XPS Graphs of (a) Survey scan of CuO@CuSe AG (b) O1s (c) Cu 2p3/2 and (d) Se 3d

We used XPS to determine the chemical composition of CuO@CuSe AG composite. The XPS survey spectrum showed Cu, Se and O peaks in the CuO@CuSe AG composite. A moment in time shows the multiple peaks around 932.4, 934.6, 942.25, 952.2 and 954.4 eV [68]. The peak at 932.4 eV is likely associated with Cu (I) oxide (Cu_2O). The peak at 934.6 eV indicates Cu (II) oxide (CuO). The peak at 942.25 eV represents the transition in the oxidation state of copper oxide. $Cu2p_{3/2}$ XPS spectra

clearly show oxidation from Cu+ to a combination of Cu+ and Cu^{+2}. The binding energy for selenium 3d core level peak of 55.1 eV confirms a lattice Se^{-2} f while the peak at 60.4 eV shows an oxidation state of selenium as shown in fig 4.3.1 (a), (b), (c) and (d). Meanwhile, the O 1 s scan revealed two dominant peaks at 532.5 and 534.8 eV consistent with C-O and O-H [69].

4.3.2 X-ray Diffraction Spectroscopy

When analyzing materials by XRD technicians use standard databases to compare diffraction patterns in order to identify crystalline phases. The lattice arrangement and all crystal parameters stem from this process. When analyzing the crystallinity of materials through XRD techniques one can determine the level of crystalline arrangement from the peak sharpness. The characteristic XRD peaks of cubic krutaite CuSe AG appear at 51°, 54° and 56°, 68°, 78° that correspond to JCPDS file No. 96901-1303 reflecting the (222), (023) and (132), (024), (043) planes. Orthorhombic spertiniite CuO shows diffraction peak patterns at 23°, 32, 37°, and 43°, 47°, 82° which correspond to planes (021), (110), (041), (131), (112), and (044) per JCPDS file No. 96-900-9158. Both copper selenide aerogel and copper oxide phases show excellent crystallinity according to their sharp peak patterns as shown in fig 4.3.2. The composite structure developed through doping led to peak detection from both CuO and CuSe AG materials. The doping of copper oxide into copper selenide aerogels results in peak position alterations because of chemical composition modifications and strain from doping. A further analysis of peak shifts against standard patterns will help determine the results. The aerogel matrix spreads peaks from some phases likely because it contains tiny crystallites and partial unorganized area [70].

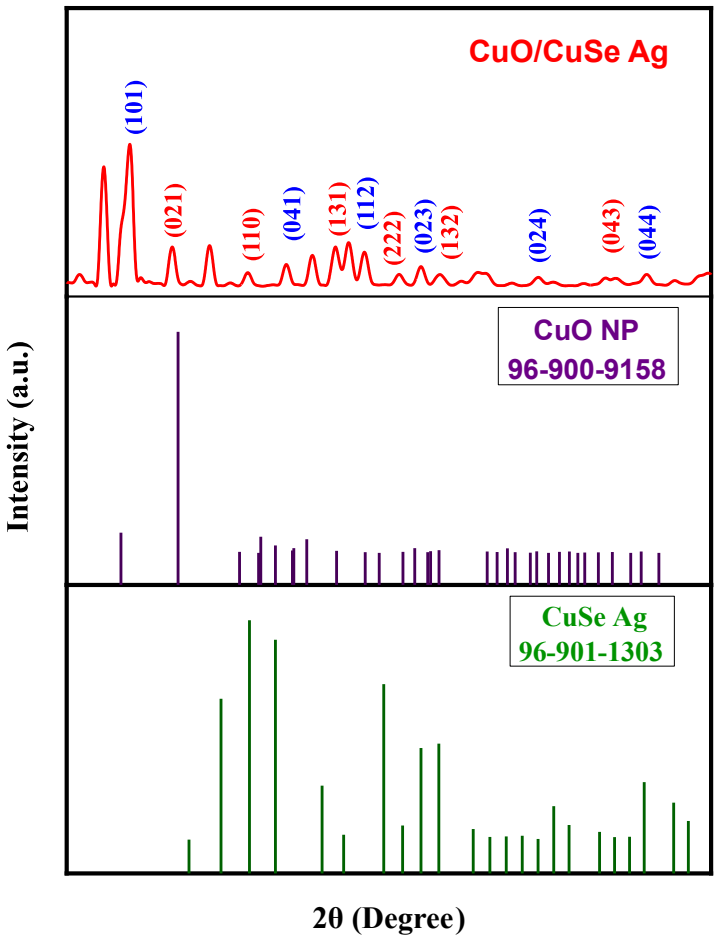

Figure 4.3.2 XRD graph of composite CuO@CuSe AG

When analyzing materials by XRD technicians use standard databases to compare diffraction patterns in order to identify crystalline phases. The lattice arrangement and all crystal parameters stem from this process. When analyzing the crystallinity of materials through XRD techniques one can determine the level of crystalline arrangement from the peak sharpness. The characteristic XRD peaks of cubic krutaite CuSe AG appear at 51°, 54° and 56°, 68°, 78° that correspond to JCPDS file No. 96901-1303 reflecting the (222), (023) and (132), (024), (043) planes. Orthorhombic spertiniite CuO shows diffraction peak patterns at 23°, 32, 37°, and 43°, 47°, 82° which correspond to planes (021), (110), (041), (131), (112), and (044) per JCPDS file No. 96-900-9158. Both copper selenide aerogel and copper oxide phases show excellent crystallinity according to their sharp peak patterns. The composite structure developed through doping led to peak detection from both CuO and CuSe AG materials. The doping of copper oxide into copper selenide aerogels results in peak

position alterations because of chemical composition modifications and strain from doping. A further analysis of peak shifts against standard patterns will help determine the results. The aerogel matrix spreads peaks from some phases likely because it contains tiny crystallites and partial unorganized area [70].

4.4 Gas Chromatography

Gas Chromatography was done to identify and quantify methanol in the CuSe AG and composite of CuO@CuSe AG

Methanol Analysis via Gas chromatography (GC)

Standard Methanol Data

Throughout multiple runs the standard methanol sample maintained its retention time at 12.82 minutes. The peak area measurement of the standard sample fell within 267,688.05–268,053.45 which proved that the GC instrument provided reliable and reproducible detection of methanol. The standard peak shape together with a tailing factor between 0.64–0.68 demonstrates the high quality of the acquired standard data.

The retention time of CuSe AG and CuO@CuSe AG matches the standard methanol peak that points to the analysis detecting methanol. The amount of detected methanol can be determined through the calibration curve obtained from the standard.

Comparison and Implications

Retention Time: Both samples had RTs nearer to the standard, confirming methanol identification.

Peak Quality: Peak symmetry shows acceptable characteristics based on the fact that the tailing factor approaches a value of 1.0 slightly better than the standard. The symmetry of peaks was satisfactory for both samples indicating proper GC function.

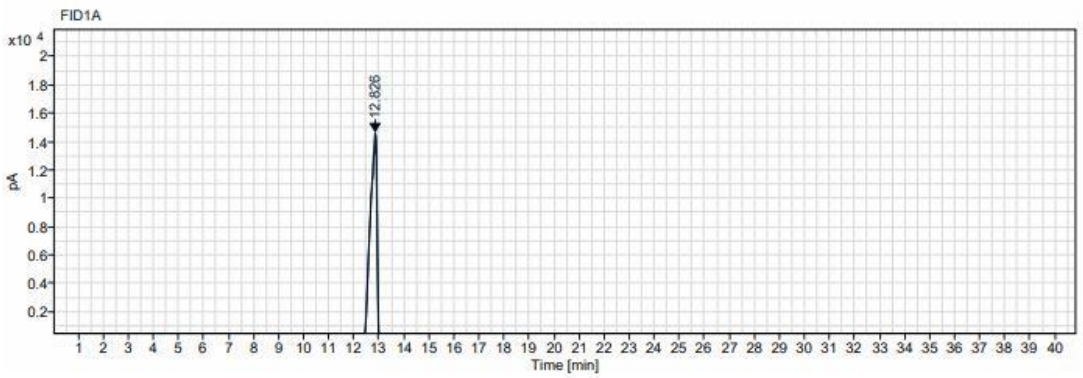

(a)

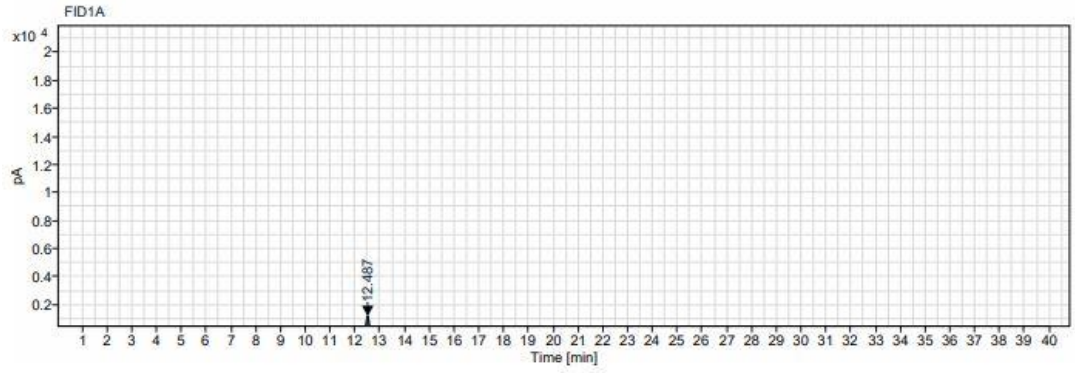

(b)

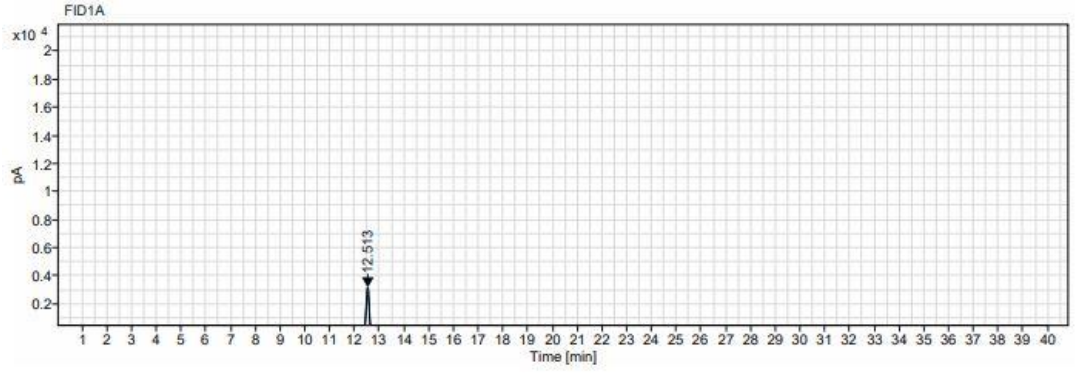

(c)

Figure 4.4 Comparison of Methanol analysis chromatogram via Gas Chromatography (a) GC methanol Standard data chromatogram (b) Methanol chromatogram CuSe AG (c) Methanol chromatogram of CuO@CuSe AG

Table 4.4 GCFID Signals data

Name	Peak Area %	RT (min)	Area	Height	Tail Factor	Theoretical Plates USP
STD Methanol 100%	100.00	12.826	267688.05	14587.00	0.67832	9606.64961
CuSe AG	100.0	12.487	49240.10	2184.60	1.07601	39797.0124
CuO/CuSe AG	100.0	12.513	152616.70	9315.99	0.95505	18346.4970

4.5 Photocatalytic CO_2 Reduction into Methanol

Research evaluated the photoreduction activity through examination of CuSe AG and CuO@CuSe AG samples under UV/visible light irradiation conditions. The photoproduction of methanol reaches its highest quantity when using CuO@CuSe AG instead of CuSe AG. By comparing different samples, it becomes clear that the attachment of CuO enhances the catalytic properties because of a strong bond and demonstrates that CuSe with CuO integration allows effective interfacial bonding between CuSe components.

The photoreaction experiments on the CuO@CuSe AG composite were conducted for 6 hours under UV ($k > 100$) and visible ($k > 100$) illumination. The absence of methanol yield during the control experiment proved that photocatalysts and light were necessary to generate a methanol production. The production of methanol through photocatalysis was measured under visible light for both CuSe AG and CuO@CuSe AG.

The rate of methanol yield was calculated by using this formula:

$$\textbf{Yield} = \frac{\text{Concentration of methanol in (ppm)} \times \text{Volume of solution (l)}}{\text{mass of catalyst (g)} \times \text{reaction time (hour)}}$$

The Quantum Efficiency or yield can be estimated by using this expression

$$\textbf{QE} = \frac{\text{number of moles of product formed} * \text{number of moles of electron required}}{\text{Number of photons absorbed by photocatalyst}} \times 100$$

$$\textbf{QE} = \frac{\text{Number of moles in mol/L} * 6 * N_A}{IE * A * T * \lambda / HC}$$

Where I_E is the light intensity (3.5729 w/cm^2), A is the irradiated area of photocatalyst (0.00321 m2), λ is the wavelength of light (>400nm in case of visible light), h is the plank's constant (6.64 *10^{-34}), C is the speed of light (3* 10^{-8}ms^{-1}), T is the time of reaction in seconds (3600s), N_A is the Avogadro's number (6.022*10^{23}).

Table 4.5 Comparison of yield of CuSe and CuO@CuSe AG

Samples	**Precursor**	**Reductant**	**Vis/UV (nm)**	**Time (h)**	**MeOH (μmolg^{-1}h^{-1})**	**QE (%)**
CuSe AG	CO_2	H_2O	400/265	6	81.057	0.083
CuO/CuSe AG	CO_2	H_2O	400/265	6	1219.63	2.56

The effect of CuO loading on copper selenide aerogel has been enshrined in the figure. The methanol yield, increases when CuO dopped into the CuSe AG. A higher dispersion of CuO nanoparticles that allow it to adsorb the maximum amount of visible light-mediated electron transition to the conduction band, a large number of light absorptions, a large number of OVs, and Schottky defects that support the photo-

mediated electron transfer and suppress the carrier charge recombination are the arguments attributed to greater electron acceptance, which lowers the probability of carriers charge recombination (e+,h). A substantial interfacial synergistic impact between CuSe AG and CuO is made possible by CuO supporting the interaction with CuSe, which leads to increased formation towards heterojunction.

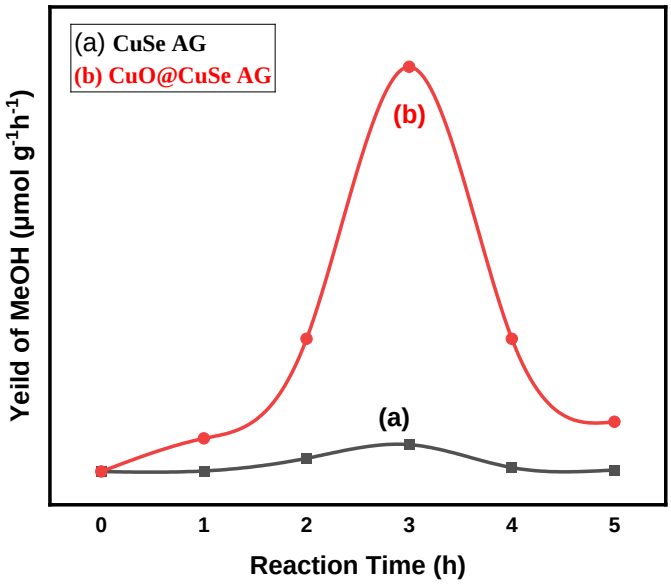

Figure 4.5 Comparison Yeild graphs of CuSe AG and CuO@CuSe AG

Photo-electric Performance Analysis

The key to effective photocatalytic photoreduction of carbon dioxide is the separation efficiency of the charge carrier produced by photocatalysis in the photocatalyst. We anticipated excellent photocatalyst performance due to the increased charge separation. Photoluminescence at room temperature was used to test the photocatalyst's separation efficiency. The enhanced intensity of the composite made from copper oxide-doped copper selenide aerogel can be attributed to the heterojunction interface between CuO and copper selenide aerogel. The exceptional performance of CuO@CuSe AG in CO_2 photoreduction is linked to its favorable photoelectric properties.

CHAPTER 5

DISCUSSION

The use of CuSe aerogel photocatalysts with co-catalysts of copper oxide (CuO) has demonstrated significant improvements towards photocatalytic levels of CO_2 reduction to methanol. The two work together to change structural and electrical parameters, which make activity better and more selective.

The previous literature presented data showing 936.33 $\mu molg^{-1}h^{-1}$ as the recorded methanol yield towards CuZnO@rGO [71]. The current research obtains efficient methanol yield values than the previously documented benchmark through the application of copper oxide-doped copper selenide aerogel catalysts. Catalytic measurements indicate the doped aerogel material shows superior efficiency when producing methanol thus reaching or surpassing records previously set for this process. This is also beneficial for application of photoreduction of CO_2 due to its simple synthesis and low-cost metals.

SEM examination indicates that the hierarchical porous structure of the aerogel has a large surface area and a large number of active sites for CO_2 reduction. FTIR spectra showed the existence of functional group (Se-O, Cu-Se and Cu-O) required for stabilizing chemical intermediates. XPS measurements verified the presence of Cu 2p3/2 and Se 3d species and the promoting electron transfer and inhibiting charge recombination by adding CuO. The bandgap of 1.5 eV (UV-Vis study) calculated from lower bandgap is obtained due to the small bandgap of CuO. By using visible light, the optimized CuO/CuSe modified aerogel surpassed many documented systems and achieved methanol production of 1219.63 $\mu mol \cdot g^{-1} \cdot h^{-1}$.

CuO acts as an electron sink, prolonging carrier lifetimes and directing electrons to active sites. CuO has been shown to stabilize the *OCHO intermediate aiding the selectivity towards methanol rather than competing products such as HCOOH2 or CO. First aligned redox potentials for the reduction of CO_2 to methanol and preserving the ability to oxidize water, a 1.5 eV bandgap is retained. The compositional complexity of the CuSe Ag framework is probably suppressing the

deactivation pathways, but more research is needed to identify which individual constituent is responsible of each possible deactivation pathway.

This system can work but more study is required to assess its scalability and industrial stability. Methanol selectivity can be tuned to further by varying CuO ratios, as well as, examining dopant (like transition metals). When implementing in conjunction with renewable energy, bulky CO_2 valorization may become more sustainable. This work demonstrates how CuSe aerogel and carefully selected co-catalysts can bridge the gap for photocatalytic applications of CO_2.

CONCLUSIONS

The photoreduction of carbon dioxide under visible light irradiation became possible through successful synthesis of copper selenide (CuSe) aerogel. The prepared aerogel reached better photocatalytic performance by producing 81.057 $\mu molg^{-1}h^{-1}$ CO_2 reduction products such as methanol. The addition of copper oxide (CuO) as a dopant to the copper selenide aerogel generated a CuO–CuSe AG composite for improvement. The introduction of copper oxide (CuO) into the copper selenide aerogel transformed the photocatalytic activity so that production amounts increased from 81.057 $\mu molg^{-1}h^{-1}$ to 1046.63 $\mu molg^{-1}h^{-1}$. The experimental data proves that CuO-doped CuSe aerogel function as an effective sustainable photocatalyst for CO_2 reduction applications therefore advancing the development of solar fuel generation and environmental remediation technologies.

The research successfully synthesized copper selenide aerogel and copper oxide-doped copper selenide aerogel for their intended use in photoreduction of CO_2. UV-Vis spectroscopy analysis showed that doping induced a major shift of light absorption toward the red spectrum from 428 nm to 564 nm. The band gap was reduced from 2.63 eV to 1.53 eV, expanded its charge carrier production potential under visible light exposure. The photoluminescence results indicated that photogenerated carrier recombination rates decreased because the emission spectrum shifted from 636.4 nm to 533.5 nm. Cu–O, Cu–Se and Se–O bonds were clearly detected in FTIR testing, while SEM revealed morphological features supporting the successful incorporation of copper oxide. XPS confirmed the chemical states and elemental composition of Cu, Se and O. The combination of results showed copper oxide doping produced structural, optical and electronic property changes which makes these materials promising for photocatalytic CO_2 reduction applications.

REFERENCES

1. Fricke J, Emmerling A. Aerogels. Journal of the American Ceramic Society. 1992;75(8):2027-35.
2. Fricke J, Tillotson T. Aerogels: production, characterization, and applications. Thin solid films. 1997;297(1-2):212-23.
3. Fricke J, Emmerling A. Aerogels—recent progress in production techniques and novel applications. Journal of Sol-Gel Science and Technology. 1998;13:299-303.
4. Schmidt M, Schwertfeger F. Applications for silica aerogel products. Journal of non-crystalline solids. 1998;225:364-8.
5. Herrmann G, Iden R, Mielke M, Teich F, Ziegler B. On the way to commercial production of silica aerogel. Journal of non-crystalline solids. 1995;186:380-7.
6. Akimov YK. Fields of application of aerogels. Instruments and experimental techniques. 2003;46:287-99.
7. Ziegler C, Wolf A, Liu W, Herrmann AK, Gaponik N, Eychmüller A. Modern inorganic aerogels. Angewandte Chemie International Edition. 2017;56(43):1320021.
8. Budtova T, Lokki T, Malakooti S, Rege A, Lu H, Milow B, Vapaavuori J, Vivod SL. Acoustic properties of aerogels: current status and prospects. Advanced Engineering Materials. 2023 Mar;25(6):2201137.
9. Jin R, Zhou Z, Liu J, Shi B, Zhou N, Wang X, Jia X, Guo D, Xu B. Aerogels for thermal protection and their application in aerospace. Gels. 2023 Jul 26;9(8):606.
10. Smirnova I, Gurikov P. Aerogels in chemical engineering: Strategies toward tailor-made aerogels. Annual review of chemical and biomolecular engineering. 2017;8(1):307-34.
11. Keshavarz L, Ghaani MR, English NJ. The importance of precursors and modification groups of aerogels in CO2 capture. Molecules. 2021;26(16):5023.
12. Gupta N, Ricci W. Processing and compressive properties of aerogel/epoxy composites. Journal of materials processing technology. 2008 Mar 3;198(1-3):178-82.
13. Sheng Z, Liu Z, Hou Y, Jiang H, Li Y, Li G, Zhang X. The rising aerogel fibers: status, challenges, and opportunities. Advanced Science. 2023 Mar;10(9):2205762.
14. Jia G, Guo J, Guo Y, Yang F, Ma Z. CO2 Adsorption Properties of Aerogel and Application Prospects in Low-carbon Building Materials: A Review. Case Studies in Construction Materials. 2024 Apr 18:e03171.
15. Randall JP, Meador MA, Jana SC. Tailoring mechanical properties of aerogels for aerospace applications. ACS applied materials & interfaces. 2011 Mar 23;3(3):61326.
16. Babiarczuk B, Lewandowski D, Kierzek K, Detyna J, Jones W, Kaleta J, Krzak J. Mechanical properties of silica aerogels controlled by synthesis parameters. Journal of Non-Crystalline Solids. 2023 Apr 15;606:122171.

17. Dorcheh AS, Abbasi MH. Silica aerogel; synthesis, properties and characterization. Journal of materials processing technology. 2008 Apr 1;199(1-3):1026.
18. Niculescu AG, Tudorache DI, Bocioagă M, Mihaiescu DE, Hadibarata T, Grumezescu AM. An updated overview of silica aerogel-based nanomaterials. Nanomaterials. 2024 Mar 4;14(5):469.
19. Yamazaki Y, Takeda H, Ishitani O. Photocatalytic reduction of CO2 using metal complexes. Journal of Photochemistry and Photobiology C: Photochemistry Reviews. 2015;25:106-37.
20. Chen X, Ye X, He J, Pan L, Xu S, Xiong C. Preparation of Fe 3+-doped TiO 2 aerogels for photocatalytic reduction of CO 2 to methanol. Journal of Sol-Gel Science and Technology. 2020;95:353-9.
21. Kumar A, Rana A, Sharma G, Sharma S, Naushad M, Mola GT, et al. Aerogels and metal–organic frameworks for environmental remediation and energy production. Environmental Chemistry Letters. 2018;16:797-820.
22. Gao B, Feng X, Zhang Y, Zhou Z, Wei J, Qiao R, Bi F, Liu N, Zhang X. Graphenebased aerogels in water and air treatment: a review. Chemical Engineering Journal. 2024 Feb 15:149604.
23. Wen M, Benabdesselam M, Beauger C. CO2 photoreduction to methanol over Nb and N co-doped TiO2 aerogel deposited CuxO. Journal of CO2 Utilization. 2024 Mar 1;81:102719.
24. El Hafdaoui H, Khallaayoun A, Ouazzani K. Activity and efficiency of the building sector in Morocco: A review of status and measures in Ifrane. AIMS Energy. 2023;11(3):454-85.
25. Pierre AC, Pajonk GM. Chemistry of aerogels and their applications. Chemical reviews. 2002;102(11):4243-66.
26. Baetens R, Jelle BP, Gustavsen A. Aerogel insulation for building applications: A state-of-the-art review. Energy and buildings. 2011;43(4):761-9.
27. Hoque KA, Sathi SA, Akter F, Akter T, Ahmed T, Ullah W, Arafin K, Rahaman MS, Shahadat HM, Imran AB, Chowdhury AN. Recent advances on photocatalytic CO2 reduction using CeO2-based photocatalysts: A review. Journal of Environmental Chemical Engineering. 2024 Jul 6:113487.
28. Pekala R. Organic aerogels from the polycondensation of resorcinol with formaldehyde. Journal of materials science. 1989;24:3221-7.
29. Ali A, Oh W-C. Catalytic reduction of CO2 to alcohol with Cu2Se-combined graphene binary nanocomposites. Fullerenes, Nanotubes and Carbon Nanostructures. 2016;24(9):555-63.
30. Song X, Li X, Zhang X, Wu Y, Ma C, Huo P, et al. Fabricating C and O codoped carbon nitride with intramolecular donor-acceptor systems for efficient photoreduction of CO2 to CO. Applied Catalysis B: Environmental. 2020;268:118736.
31. Chen P, Zhang Y, Zhou Y, Dong F. Photoelectrocatalytic carbon dioxide reduction: Fundamental, advances and challenges. Nano Materials Science. 2021;3(4):344-67.

32. Sundar D, Liu C-H, Anandan S, Wu JJ. Photocatalytic CO2 conversion into solar fuels using carbon-based materials—a review. Molecules. 2023;28(14):5383.
33. Qin Y, Dong G, Zhang L, Li G, An T. Highly efficient and selective photoreduction of CO2 to CO with nanosheet g-C3N4 as compared with its bulk counterpart. Environmental Research. 2021;195:110880.
34. Elakkiya R, Maduraiveeran G. Hierarchical three-dimensional copper selenide nanocube microelectrodes for improved carbon dioxide reduction reactions. Sustainable Energy & Fuels. 2021;5(24):6430-40.
35. Lu Y, Wu D, Qin Y, Xie Y, Ling Y, Ye H, et al. Facile construction of BiOBr/CoAl-LDH heterojunctions with suppressed Z-axis growth for efficient photoreduction of CO2. Separation and Purification Technology. 2022;302:122090.
36. Karamian E, Sharifnia S. On the general mechanism of photocatalytic reduction of CO2. Journal of CO2 Utilization. 2016;16:194-203.
37. Jiang G, Wang J, Li N, Hübner R, Georgi M, Cai B, et al. Self-supported threedimensional quantum dot aerogels as a promising photocatalyst for CO2 reduction. Chemistry of Materials. 2022;34(6):2687-95.
38. Wu Z, Wu H, Cai W, Wen Z, Jia B, Wang L, et al. Engineering bismuth–tin interface in bimetallic aerogel with a 3D porous structure for highly selective electrocatalytic CO2 reduction to HCOOH. Angewandte Chemie. 2021;133(22):12662-7.
39. Xiao X, Xu Y, Lv X, Xie J, Liu J, Yu C. Electrochemical CO2 reduction on copper nanoparticles-dispersed carbon aerogels. Journal of colloid and interface science. 2019;545:1-7.
40. Sun X, Zhu Q, Kang X, Liu H, Qian Q, Zhang Z, et al. Molybdenum–bismuth bimetallic chalcogenide nanosheets for highly efficient electrocatalytic reduction of carbon dioxide to methanol. Angewandte Chemie. 2016;128(23):6883-7.
41. Yang D, Zhu Q, Chen C, Liu H, Liu Z, Zhao Z, et al. Selective electroreduction of carbon dioxide to methanol on copper selenide nanocatalysts. Nature communications. 2019;10(1):677.
42. Le M, Ren M, Zhang Z, Sprunger PT, Kurtz RL, Flake JC. Electrochemical reduction of CO2 to CH3OH at copper oxide surfaces. Journal of the Electrochemical Society. 2011;158(5):E45.
43. Lu L, Sun X, Ma J, Yang D, Wu H, Zhang B, et al. Highly efficient electroreduction of CO2 to methanol on palladium–copper bimetallic aerogels. Angewandte Chemie. 2018;130(43):14345-9.
44. Kalebaila KK, Brock SL. Lead selenide nanostructured aerogels and xerogels. Zeitschrift für anorganische und allgemeine Chemie. 2012;638(15):2598-603.
45. Zhang Z, Jiang S, Lai Y, Li J, Song J, Li J. Selenium sulfide@ mesoporous carbon aerogel composite for rechargeable lithium batteries with good electrochemical performance. Journal of power sources. 2015;284:95-102.
46. Gash AE, Tillotson TM, Satcher Jr JH, Hrubesh LW, Simpson RL. New sol–gel synthetic route to transition and main-group metal oxide aerogels using inorganic salt precursors. Journal of Non-Crystalline Solids. 2001;285(1-3):22-8.

47. Hüsing N, Schubert U. Aerogels—airy materials: chemistry, structure, and properties. Angewandte Chemie International Edition. 1998 Feb 2;37(1-2):22-45.
48. Pedroso M, Flores-Colen I, Silvestre JD, Gomes MG, Hawreen A, Ball RJ. Synergistic effect of fibres on the physical, mechanical, and microstructural properties of aerogel-based thermal insulating renders. Cement and Concrete Composites. 2023 May 1;139:105045.
49. Jadhav S, Sarawade P. Recent Advances Prospective of Reinforced Silica Aerogel Nanocomposites and Their Applications. European Polymer Journal. 2024 Jan 17:112766.
50. Freitas PA, González-Martínez C, Chiralt A. Influence of the cellulose purification process on the properties of aerogels obtained from rice straw. Carbohydrate Polymers. 2023 Jul 15;312:120805.
51. Sheng Z, Liu Z, Hou Y, Jiang H, Li Y, Li G, Zhang X. The rising aerogel fibers: status, challenges, and opportunities. Advanced Science. 2023 Mar;10(9):2205762.
52. Gao B, Feng X, Zhang Y, Zhou Z, Wei J, Qiao R, Bi F, Liu N, Zhang X. Graphene based aerogels in water and air treatment: a review. Chemical Engineering Journal. 2024 Feb 15:149604.
53. Han L, Chen S, Li H, Dong Y, Wang CA, Li J. Rapid and inexpensive synthesis of liter-scale SiC aerogels. Nature Communications. 2024 Aug 13;15(1):6959.
54. Wu X, Xia Y, Shen X, Cui S, Chen X, Koudama TD. New insight into efficient photocatalytic CO2 reduction without any sacrifice agent over the novel hierarchical structured SiOC whisker aerogel. Journal of Alloys and Compounds. 2023 Oct 25;961:171005.
55. Saravanan P, Elangovan K, Campos CH, Sanhueza-Gómez F, Annamalai P, Ramakrishnan K, Mangalaraja RV. Aerogels and carbon-based materials for photoelectrocatalytic CO2 reduction into solar fuels. InMaterials Technology for the Energy and Environmental Nexus, Volume 2 2023 Nov 1 (pp. 4-1). Bristol, UK: IOP Publishing.
56. Tseng IH, Chang WC, Wu JC. Photoreduction of CO2 using sol–gel derived titania and titania-supported copper catalysts. Applied Catalysis B: Environmental. 2002 Apr 8;37(1):37-48.
57. Shu R, Xu L, Guan Y. Preparation of cellulose derived carbon/reduced graphene oxide composite aerogels for broadband and efficient microwave dissipation. Journal of Colloid and Interface Science. 2024 Dec 1;675:401-10.
58. Liu Y, Shang J, Zhu T. Effects of N, S doping on a graphene oxide aerogel for adsorption and photocatalytic reduction of carbon dioxide. Journal of Materials Chemistry C. 2024.
59. Tang H, Chen ZA, Wu M, Li S, Ye Z, Zhi M. Au-CeO2 composite aerogels with tunable Au nanoparticle sizes as plasmonic photocatalysts for CO2 reduction. Journal of colloid and interface science. 2024 Jan 1;653:316-26.
60. Liu, H., Xia, Y., Dong, Y., Hao, Z., Sun, F., Yue, B., ... & Su, Z. (2025). Multifunctional graphene aerogels produced by protonation enhanced Schottky heterojunction interface effect. *Applied Surface Science*, *680*, 161323.

61. Liu X, Su C, Zhong Y, Zhu X, Wu Z, Cui S. High entropy (LaCeSmEuNd) 2Zr2O7 ceramic aerogel with low thermal conductivity and excellent structural heat resistance. Journal of the European Ceramic Society. 2022 Oct 1;42(13):5964-72.
62. Hu H, Ge X, Deng C, Sun M, Xuan H, Zhang K. Copper selenide (CuSe and Cu2Se) nanocrystals: Controllable synthesis through a facile ultrasonic chemical route. Asian Journal of Chemistry. 2013 Jul 1;25(10):5516.
63. Flores-Rojas E, Samaniego-Benítez JE, Serrato R, García-García A, Ramírez-Bon R, Ramírez-Aparicio J. Transformation of nanostructures Cu2O to Cu3Se2 through different routes and the effect on photocatalytic properties. ACS omega. 2020 Aug 3;5(32):20335-42.
64. Sonia S, Kumar PS, Mangalaraj D, Ponpandian N, Viswanathan CJ. Influence of growth and photocatalytic properties of copper selenide (CuSe) nanoparticles using reflux condensation method. Applied surface science. 2013 Oct 15;283:802-7.
65. Sakane S, Miwa S, Miura T, Munakata K, Ishibe T, Nakamura Y, Tanaka H. Thermoelectric properties of Pedot: PSS containing connected copper selenide nanowires synthesized by the photoreduction method. ACS omega. 2022 Sep 5;7(36):32101-7.
66. Singh SC, Li H, Yao C, Zhan Z, Yu W, Yu Z, Guo C. Structural and compositional control in copper selenide nanocrystals for light-induced self-repairable electrodes. Nano Energy. 2018 Sep 1;51:774-85.
67. Uma B, Anantharaju KS, Surendra BS, Gurushantha K, More SS, Meena S, Hemavathi B, Murthy HA. Influence of Ag on the structural, electrochemical, antibacterial, and photocatalytic performance of the (CuO–Cu2O) Cu nanocomposite. ACS omega. 2023 Mar 10;8(11):9947-61.
68. Li H, Lei Y, Huang Y, Fang Y, Xu Y, Zhu L, Li X. Photocatalytic reduction of carbon dioxide to methanol by Cu2O/SiC nanocrystallite under visible light irradiation. Journal of Natural gas chemistry. 2011 Mar 1;20(2):145-50.
69. Karuppasamy K, Vikraman D, Hussain S, Veerasubramani GK, Santhoshkumar P, Lee SH, Bose R, Kathalingam A, Kim HS. Unveiling a binary metal selenide composite of CuSe polyhedrons/CoSe2 nanorods decorated graphene oxide as an active electrode material for high-performance hybrid supercapacitors. Chemical Engineering Journal. 2022 Jan 1;427:131535.
70. Mata-Padilla JM, Ledón-Smith JÁ, Pérez-Alvarez M, Cadenas-Pliego G, BarrigaCastro ED, Pérez-Camacho O, Cabello-Alvarado CJ, Silva R. Synthesis and Superficial Modification “In Situ” of Copper Selenide (Cu2-x Se) Nanoparticles and Their Antibacterial Activity. Nanomaterials. 2024 Jul 4;14(13):1151.
71. Kubovics M, Trigo A, Sánchez A, Marbán G, Borrás A, Moral-Vico J, López-Periago AM, Domingo C. Role of graphene oxide aerogel support on the CuZnO catalytic activity: enhancing methanol selectivity in the hydrogenation reaction of CO2. ChemCatChem. 2022 Sep 20;14(18):e202200607.

Report:Synthesis Of Copper Selenide Aerogel For Photoreduction Of Carbon Dioxide (HAMDA RAFIQUE)

ORIGINALITY REPORT

7%	1%	6%	0%
SIMILARITY INDEX	INTERNET SOURCES	PUBLICATIONS	STUDENT PAPERS

PRIMARY SOURCES

1	Xin Li, Jiaguo Yu, Mietek Jaroniec, Xiaobo Chen. " Cocatalysts for Selective Photoreduction of CO into Solar Fuels ", Chemical Reviews, 2019 Publication	1%
2	Khondaker Afrina Hoque, Sharmin Ara Sathi, Farjana Akter, Tania Akter et al. "Recent Advances on Photocatalytic CO2 reduction using CeO2-based Photocatalysts: A Review", Journal of Environmental Chemical Engineering, 2024 Publication	1%
3	Hao Tang, Zi Ang Chen, Muchen Wu, Shunbo Li, Ziran Ye, Mingjia Zhi. "Au-CeO2 Composite Aerogels with Tunable Au Nanoparticle Sizes as Plasmonic Photocatalysts for CO2 Reduction", Journal of Colloid and Interface Science, 2023 Publication	<1%
4	Guanhua Jia, Jiming Guo, Yuanyuan Guo, Fengling Yang, Zhibin Ma. "CO2 adsorption properties of aerogel and application prospects in low-carbon building materials: A review", Case Studies in Construction Materials, 2024 Publication	<1%
5	Vinayak G. Parale, Taehee Kim, Haryeong Choi, Varsha D. Phadtare, Rushikesh P. Dhavale, Kazuyoshi Kanamori, Hyung-Ho	<1%

Scanned with CamScanner